



LAWRENCE
LIVERMORE
NATIONAL
LABORATORY

Progress in snowflake divertor research in DIII-D, NSTX and NSTX-U.

V. A. Soukhanovskii

October 27, 2016

58th Annual Meeting of the APS Division of Plasma Physics
San Jose, CA, United States
October 31, 2016 through November 4, 2016

Disclaimer

This document was prepared as an account of work sponsored by an agency of the United States government. Neither the United States government nor Lawrence Livermore National Security, LLC, nor any of their employees makes any warranty, expressed or implied, or assumes any legal liability or responsibility for the accuracy, completeness, or usefulness of any information, apparatus, product, or process disclosed, or represents that its use would not infringe privately owned rights. Reference herein to any specific commercial product, process, or service by trade name, trademark, manufacturer, or otherwise does not necessarily constitute or imply its endorsement, recommendation, or favoring by the United States government or Lawrence Livermore National Security, LLC. The views and opinions of authors expressed herein do not necessarily state or reflect those of the United States government or Lawrence Livermore National Security, LLC, and shall not be used for advertising or product endorsement purposes.

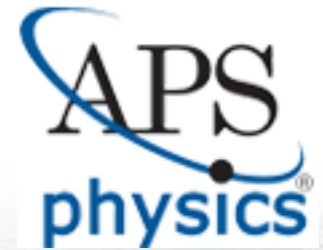
Progress in snowflake divertor research in DIII-D, NSTX and NSTX-U.

V. A. Soukhanovskii

Poster TP10.00068

58th Annual Meeting of the APS Division of Plasma Physics

Monday–Friday, October 31–November 4 2016; San Jose, California



Co-authors and Acknowledgements

S. L. Allen, M. E. Fenstermacher, O. Izacard, C. J. Lasnier, M. A. Makowski, A. G. McLean, W. H Meyer, D. D. Ryutov, F. Scotti, *LLNL*;

E. Kolemen, P. Vail, *Princeton U*;

G. P. Canal, *GA/ORAU*,

D. Eldon, R. J. Groebner, A. W. Hyatt, A. W. Leonard, T. H. Osborne, *General Atomics*;

R. E. Bell, A. Diallo, S. P. Gerhardt, S. Kaye, B. P. LeBlanc, J. E. Menard, M. Podesta, *PPPL*

This work is supported by the US DOE under DE-AC52-07NA27344, DE-AC02-09CH11466, DE-FC02-04ER54698.



Outline

1. Introduction and previous results
2. Magnetic feedback control developments
3. Core and pedestal analysis of H-mode plasmas with the snowflake divertor
4. Edge localized modes with the snowflake divertor
5. Radiative snowflake divertor studies with CD₄ injection
6. Preparation for NSTX-U experiments

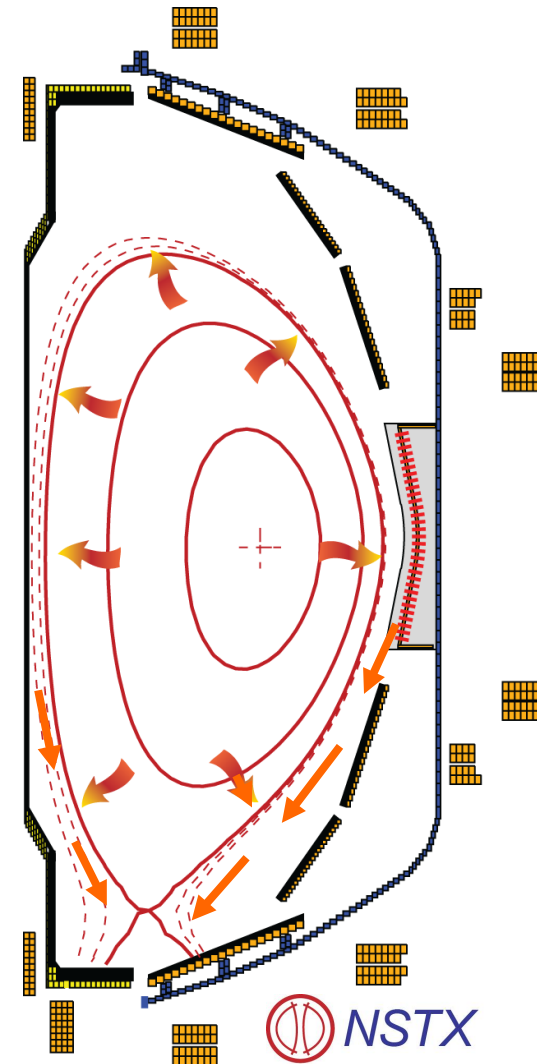
Significant gaps exist between present divertor solutions and future device requirements

■ Critical divertor tasks

- Power exhaust
- D/T and He pumping
- Impurity source reduction
- Impurity screening

■ Outstanding issues

- Steady-state heat flux
 - Technological limit $q_{peak} \leq 5-15 \text{ MW/m}^2$
 - ITER: $q_{peak} \leq 10 \text{ MW/m}^2$ (Mitigated)
 - DEMO: $q_{peak} \leq 150 \text{ MW/m}^2$ (Unmitigated)
- ELM energy, target peak temperature
 - Melting limit $0.1-0.5 \text{ MJ/m}^2$
 - DEMO: Unmitigated, $\geq 10 \text{ MJ/m}^2$
- Impurity erosion
 - Divertor target $T_e < 5-10 \text{ eV}$



Divertor strike point heat flux mitigation using radiated power loss and magnetic / PFC geometry

$$q_{peak} \simeq \frac{P_{div}}{A_{wet}} = \frac{P_{SOL}(1 - f_{rad})f_{geo}}{2\pi R_{SP}f_{exp}\lambda_{q\parallel}}$$

Radiated power loss
Increase via V_{div} , L_{\parallel}

Poloidal target inclination,
up-down, in-out fractions,
 N divertors

Increase plasma-wetted
area

Increase divertor area at
large R_{SP}

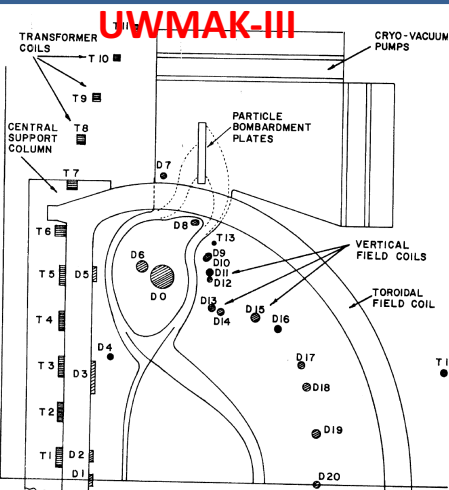
Increase $\lambda_{q\parallel}$ via
increased
radial
transport

Increase
plasma-wetted
area via
increasing f_{exp}

- Divertor physics is inherently 2D or even 3D
 - Parallel / cross-field transport and turbulence
 - Radiation front (detachment) stability
 - Neutral pressure / density distribution

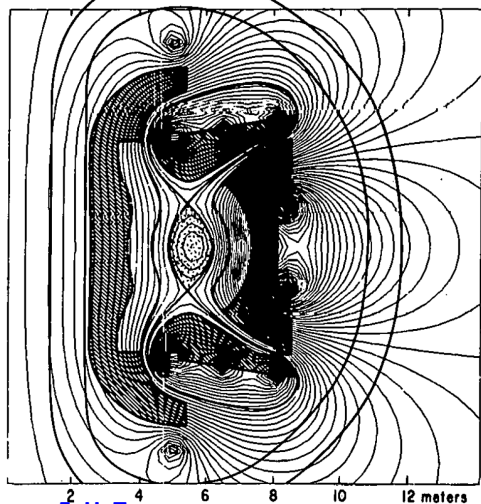
- Important engineering aspect – divertor coil layout

Focus on magnetic geometry since early days of tokamak studies. Some examples (R_{SP} , L_{II} , f_{exp}) ...



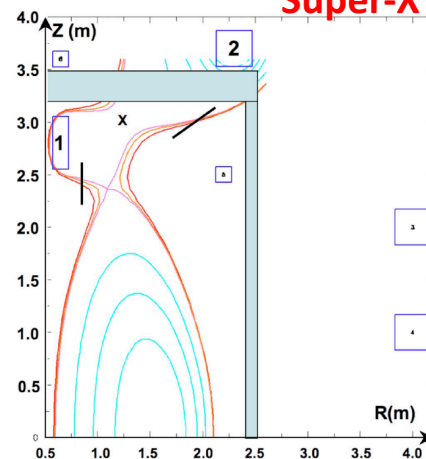
B. Badger et.al, U. Wisc. Report UWFD-150, 1975

Double-null with long legs

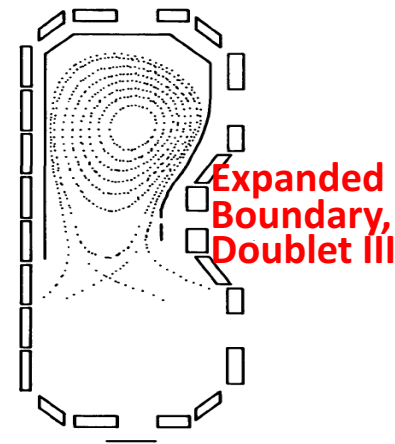


F. H. Tenney, PPPL Report 1284, 1976

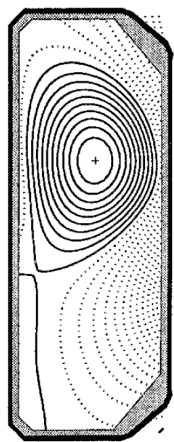
Super-X



P. M. Valanju et.al, Phys. Plasmas 16, 056110 (2009)

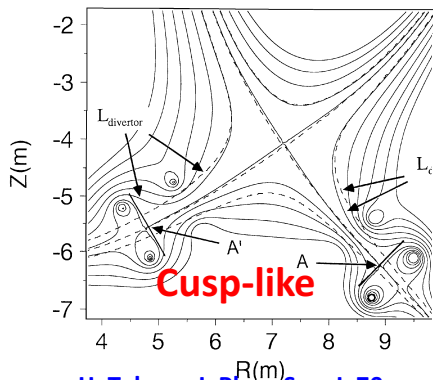


N. Ohyabu et. al, Nucl. Fusion 5 519 (1981)



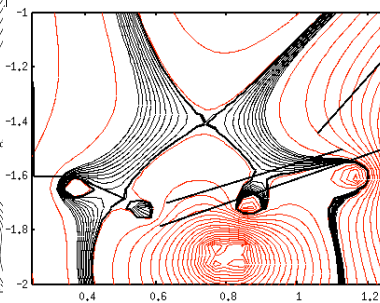
TCV

R. A. Pitts et. al, JNM 290-293, 2001, 940

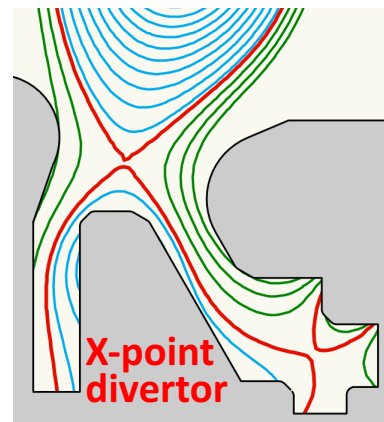


H. Takase, J. Phys. Soc. J. 70, 609, 2001

X-divertor

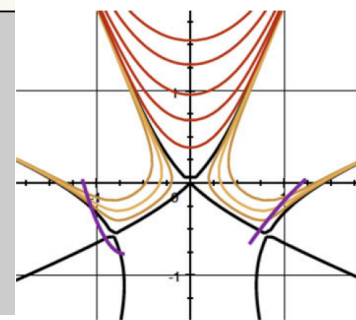


M. Kotschenreuther et. al, IAEA FEC 2004; Phys. Plasmas 14, 072502 (2007)



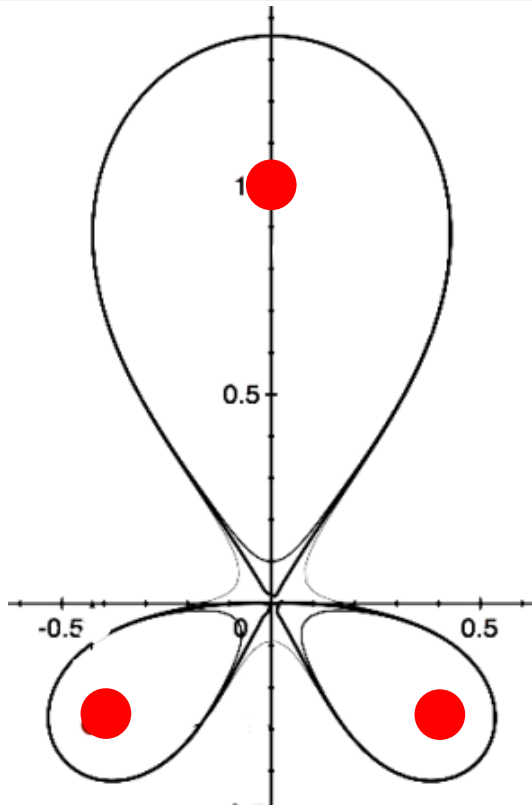
B. LaBombard et.al, NF 55 (2015) 053020

Super-cusp with Remote coils



D. D. Ryutov, J. Plasma Phys. 2015, 81, 495810516

Snowflake divertor configuration as a tokamak divertor power exhaust concept



D. D. Ryutov, PoP 14, 064502 2007;
PPCF 54, 124050 (2012)

- **Snowflake, 2nd order null**

- $B_p \sim 0$, $grad B_p \sim 0$

- (Cf. first-order null: $B_p \sim 0$)

- $B_p(r) \sim r^2$ (Cf. first-order null: $B_p \sim r$)

- Four divertor legs

- **Geometry benefits**

- Higher edge magnetic shear

- Larger plasma wetted-area A_{wet} (f_{exp})

- Larger parallel connection length $L_{||}$

- Larger effective divertor volume V_{div}

To maximize geometry benefits: $d_{xx} \leq a (\lambda_q / a)^{1/3}$

- **Transport benefits**

- High convection zone with radius D^*

- Power sharing over four strike points

- Enhanced radial transport (larger l_q)

To maximize sharing: $d_{xx} \leq D^* \sim a (a \beta_{pm} / R)^{1/3}$

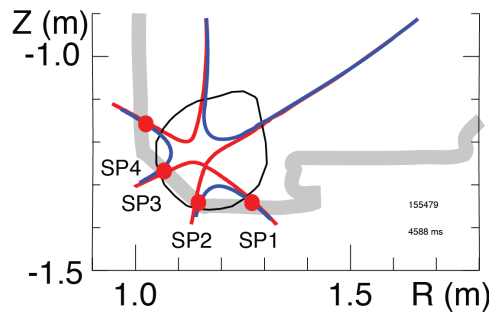
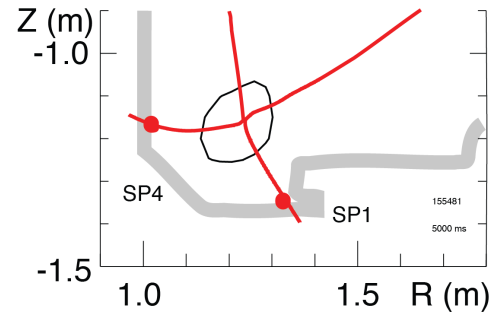
Snowflake configurations obtained in NSTX and DIII-D using existing PF coils



Standard

Snowflake

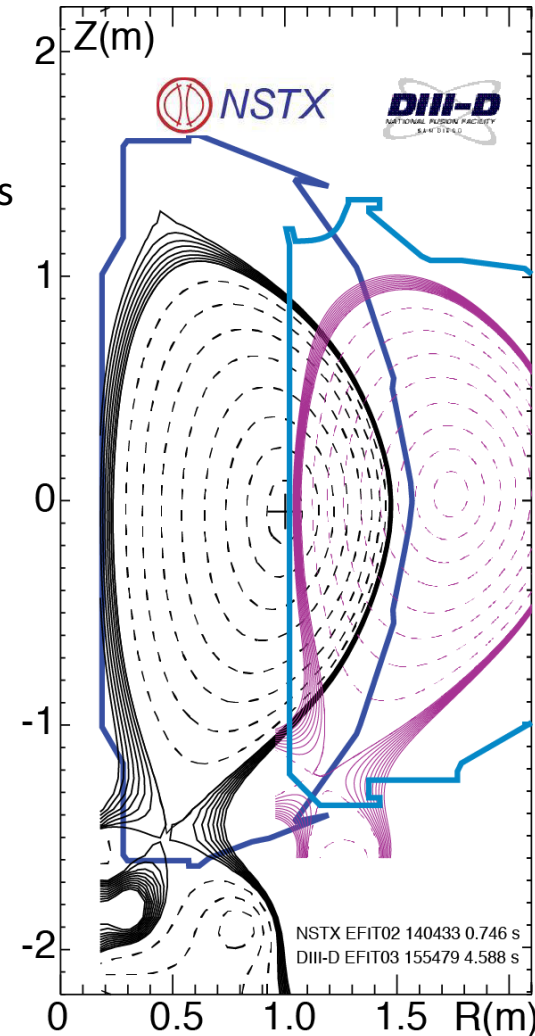
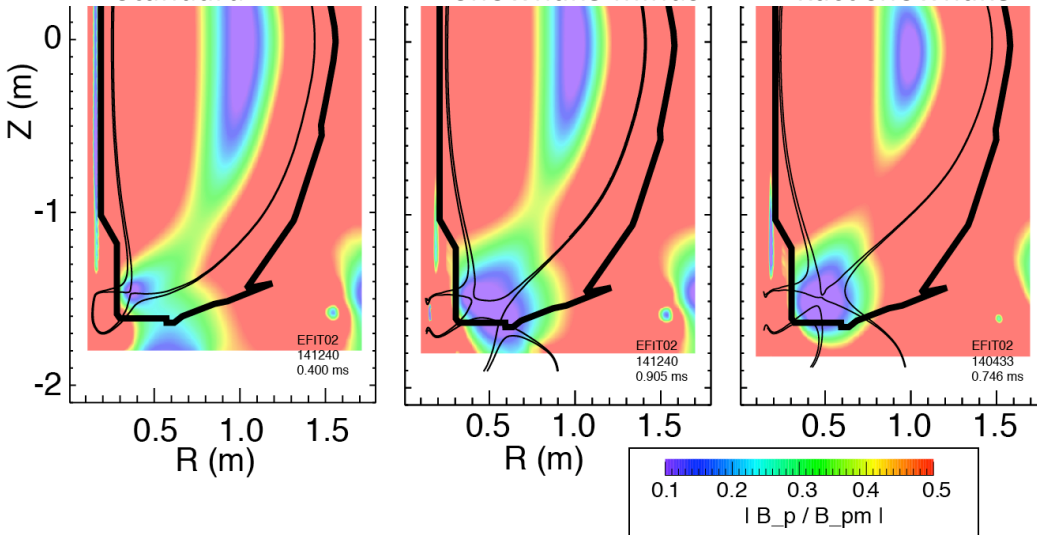
- NSTX
 - $I_p=0.8-1.0$ MA
 - $B_t \leq 0.45$ T
 - 3 divertor coils
 - SF for 0.5 s
- DIII-D
 - $I_p=0.8-1.0$ MA
 - $B_t=2$ T
 - 3 divertor coils
 - SF for 2-3 s



Standard

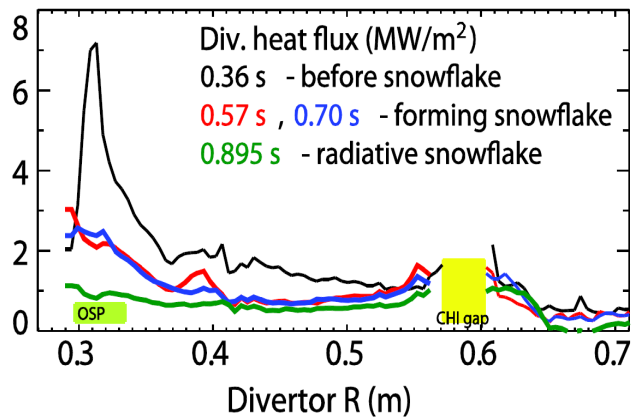
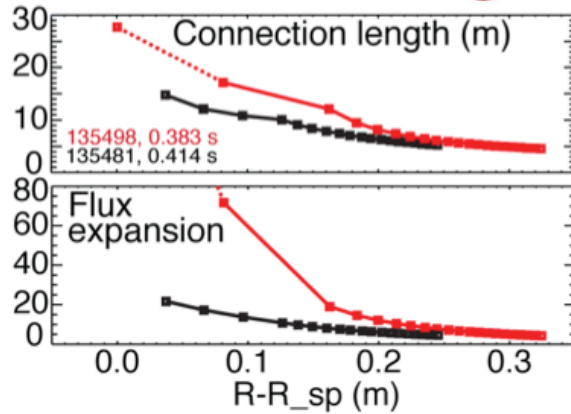
Snowflake-minus

Exact snowflake

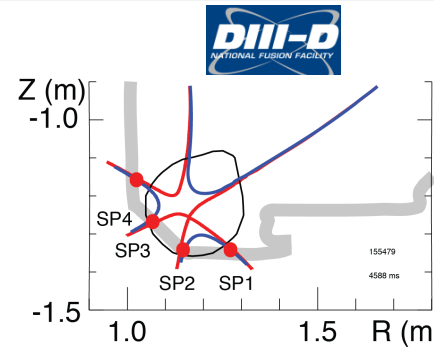


Peak divertor heat flux significantly reduced due to snowflake divertor geometry effects

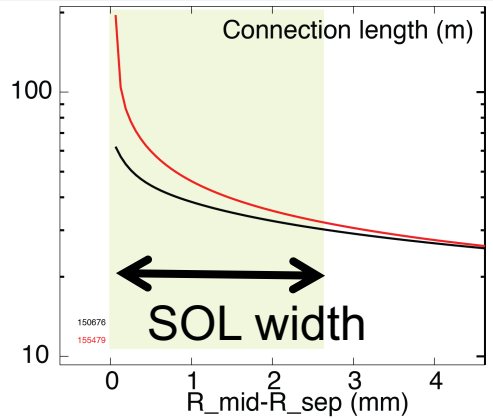
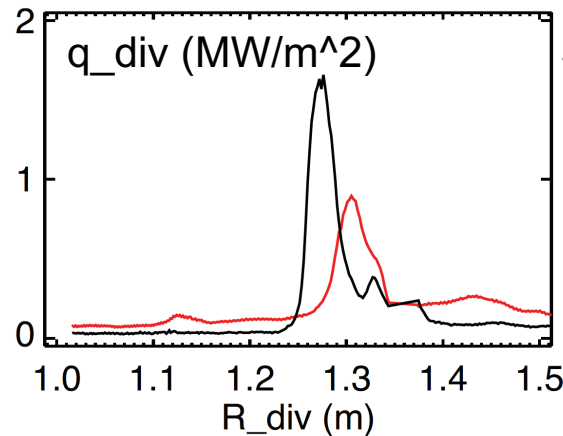
Standard **Snowflake** 



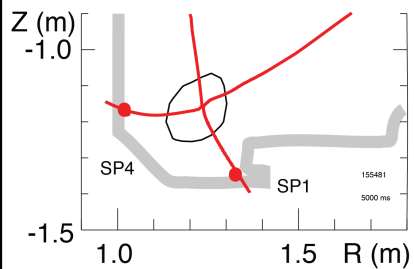
- Due to geometry and radiation



Snowflake



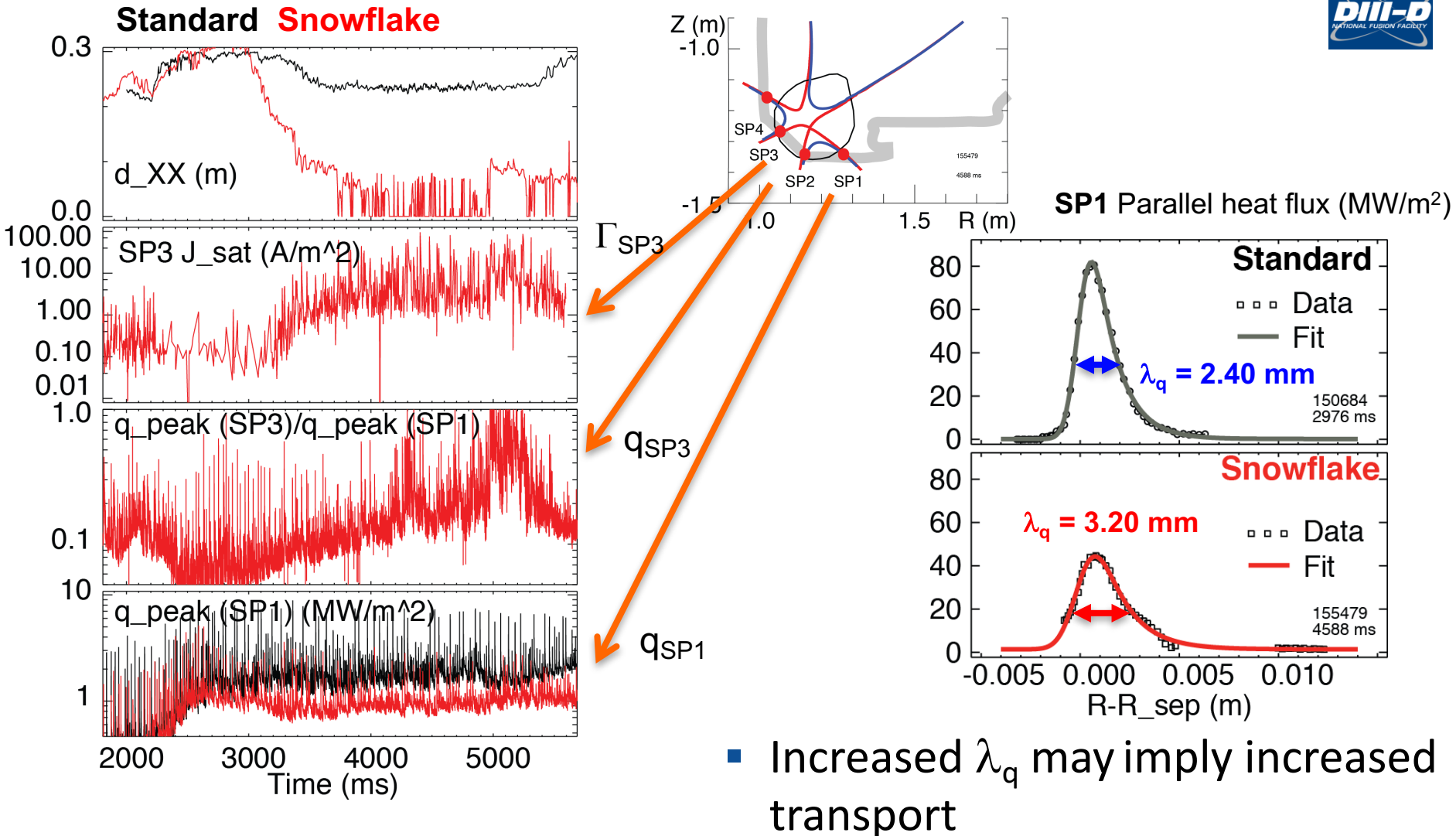
SOL width



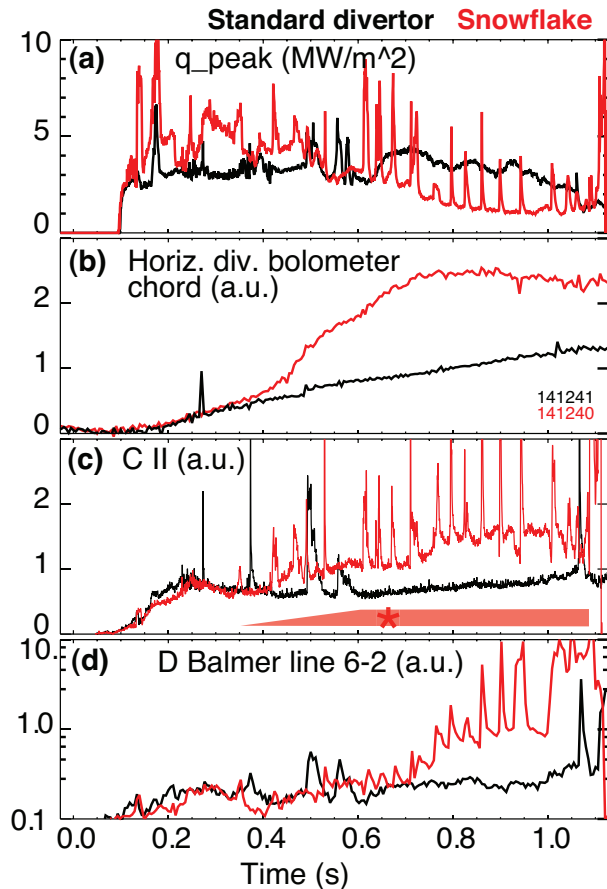
Standard

- Flux expansion increased $\sim 20\%$
- $L_{||}$ increased by 20-60% over SOL width
- Divertor heat flux reduced $\sim 40\%$

Snowflake divertor enables power and particle sharing over multiple strike points



Snowflake configuration favorably affects divertor radiation and detachment

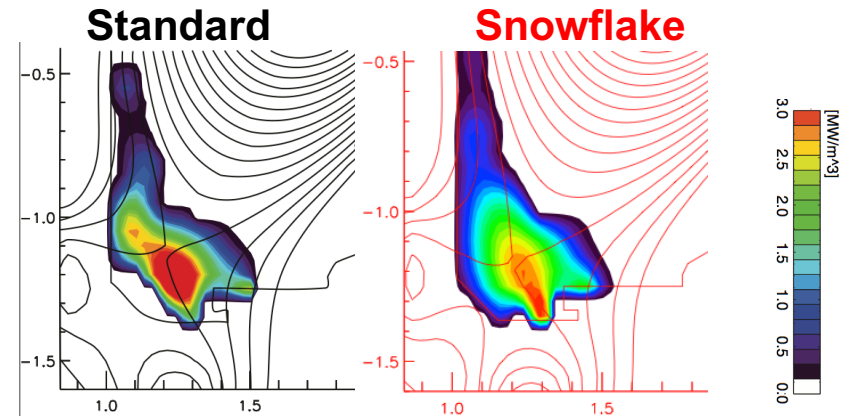
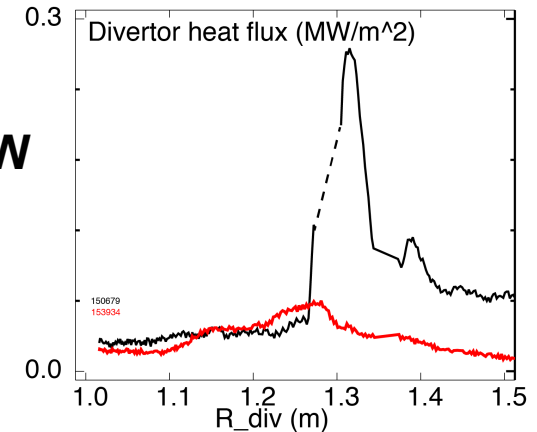


$P_{\text{SOL}} = 2-3 \text{ MW}$



$P_{\text{SOL}} = 3-4 \text{ MW}$

Radiative Standard Radiative Snowflake



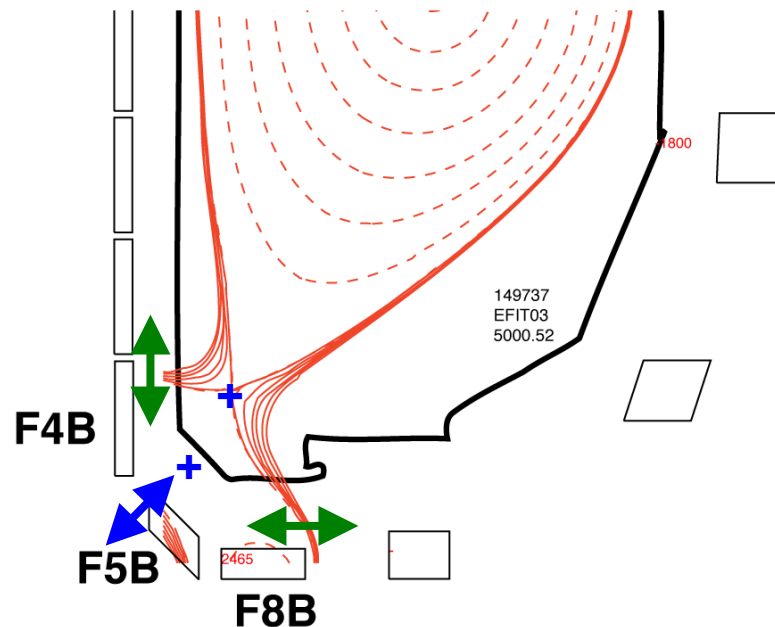
- Natural partial detachment in NSTX snowflake otherwise inaccessible with standard divertor

- Broader radiated power distribution, nearly complete power detachment in DIII-D



Continuing development of real-time snowflake configuration control

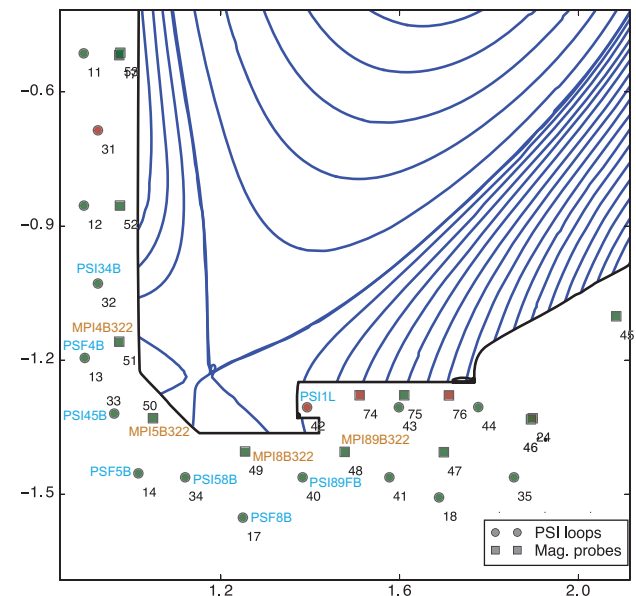
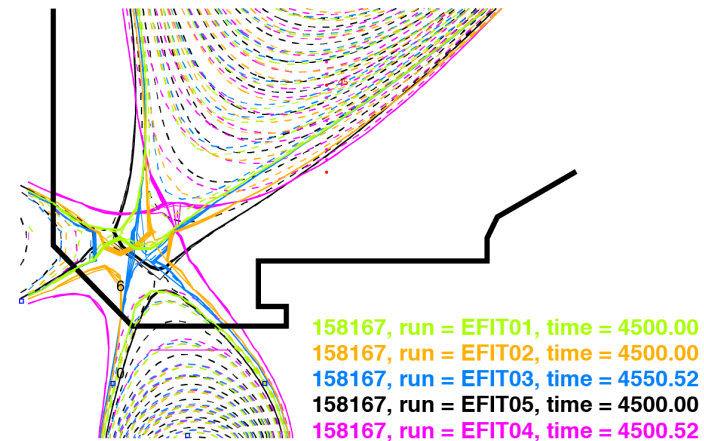
- Statement of problem - need to control
 - positions and orientation of two nulls
 - general null and strike point positions
- Grad-Shafranov equilibria modeling of possible configurations
- Present approach
 - Use rtEFIT for B_r and B_z (limited spatial resolution 65x65 grid)
 - Use B_r and B_z with Makowski's algorithm to infer null positions
 - Problem may be underdetermined
 - Limited success at DIII-D with small inter-null distances
- Inner and outer strike point positions controlled by PCS using F4B and F8B coils
- Secondary null-point formed and pushed in using F5B



P. Vail,
NP10.00008

Progress made in real-time control but several issues are still outstanding

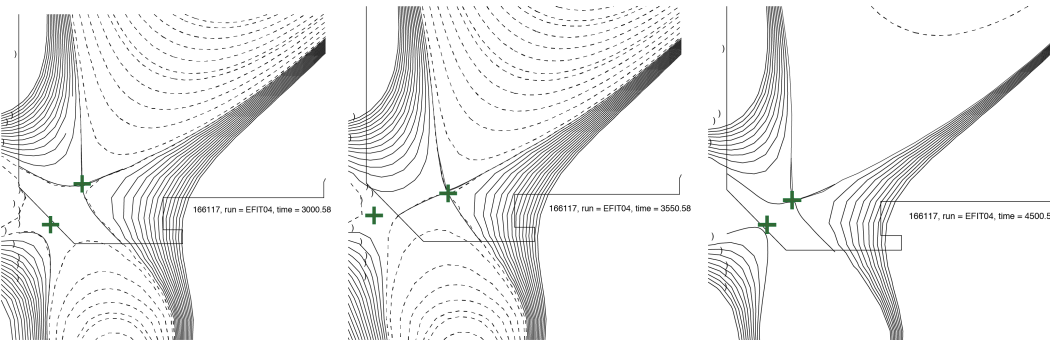
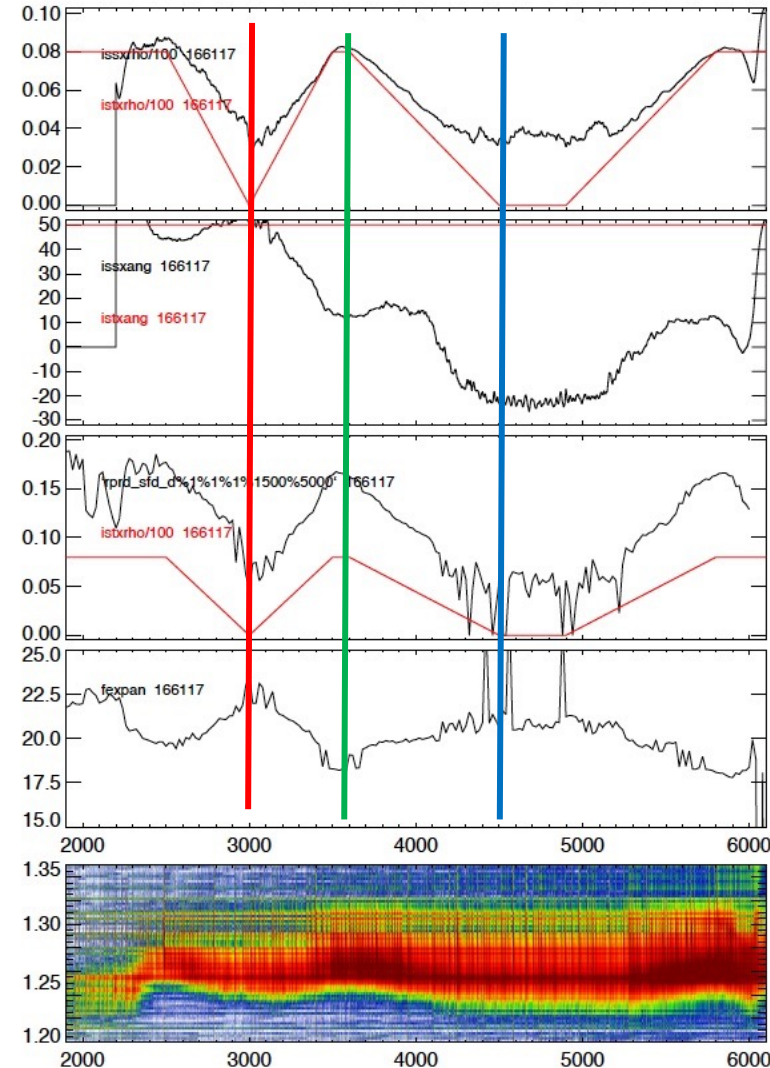
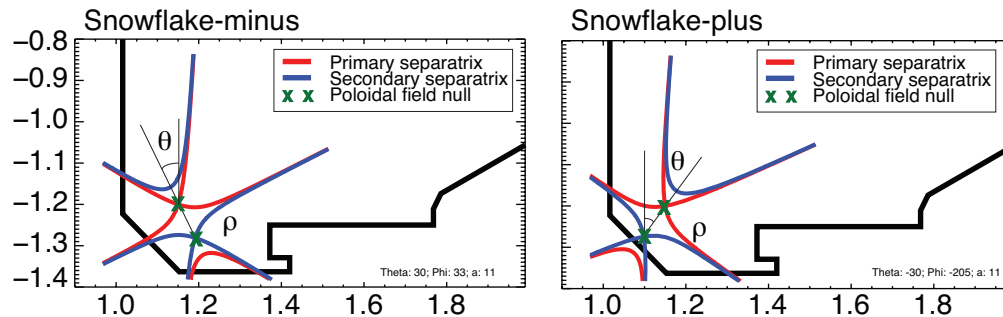
- Often heat flux footprint and divertor impurity emission distribution from cameras differ from expectations from equilibria
- Often EFIT01, EFIT02 and kinetic EFIT show different equilibria
 - JT (magnetics) vs MSE (q-profile)
 - q profile affected by SF configuration
- rtEFIT is presently 65x65
 - Additional magnetic sensors for additional divertor flux constraints ?
- Near-term plan – rtEFIT
 - Consider improvements to Makowski's algorithm
 - Study how EFIT constraints affect equilibria and snowflakes
- Consider direct sensor-based control
 - Additional magnetic sensors for additional divertor flux constraints ?



Progress made in real-time control but several issues are still outstanding

- Inter-null distance control works
- Angle control does not work

P. Vail,
NP10.00008

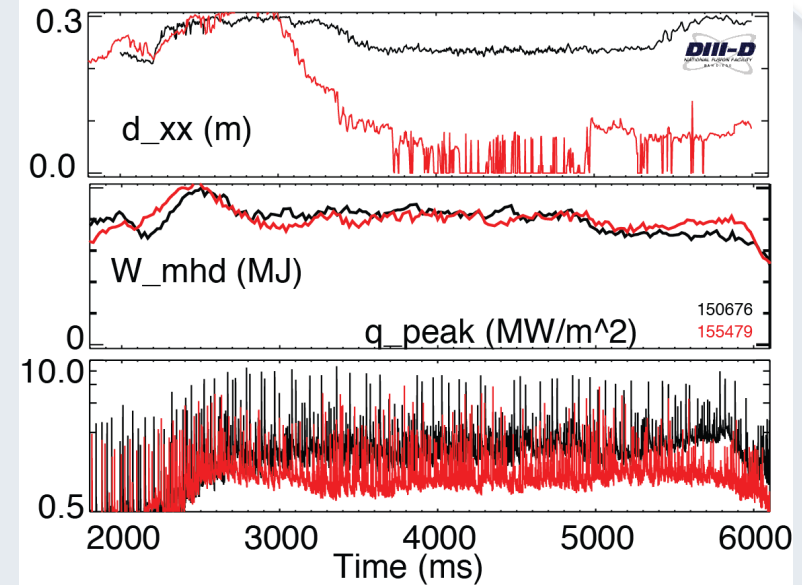
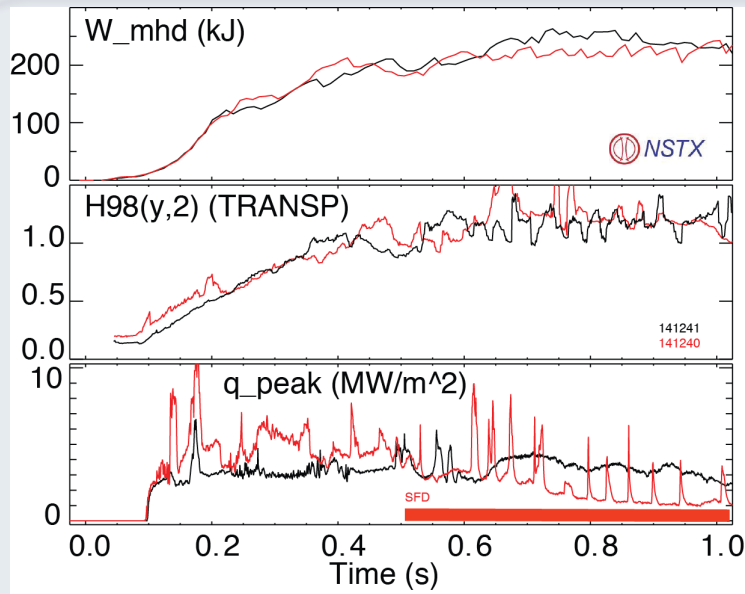


3000 ms

3550 ms

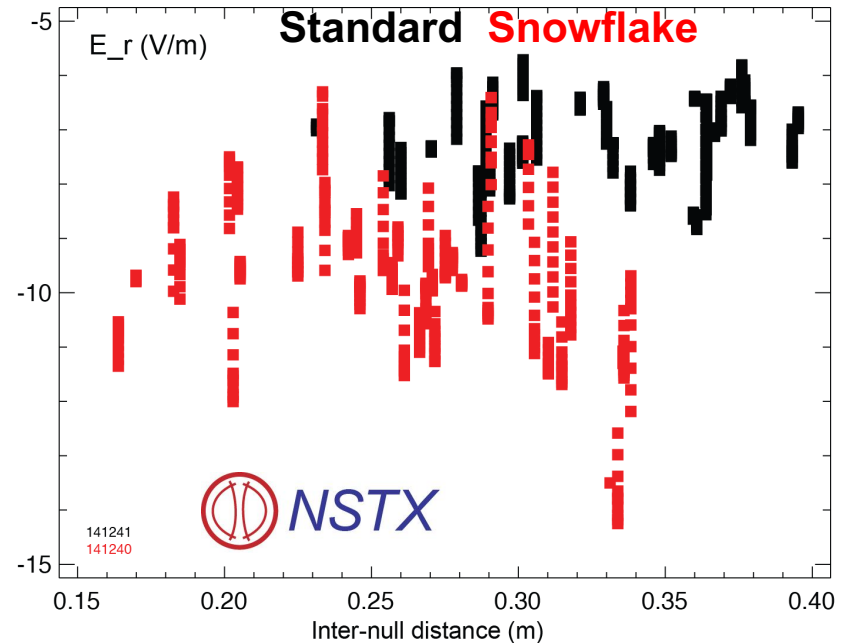
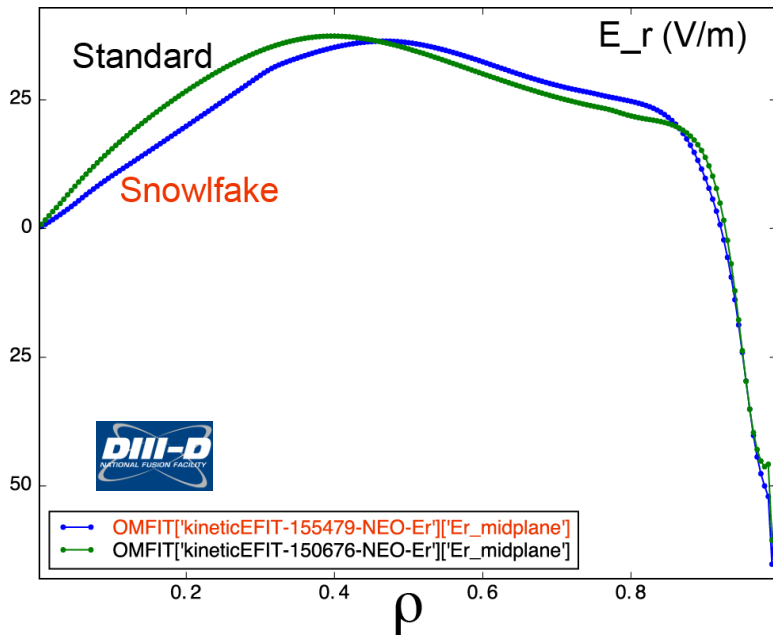
4500 ms

Spatially extended region of very low B_p may affect pedestal stability, transport and ELMs



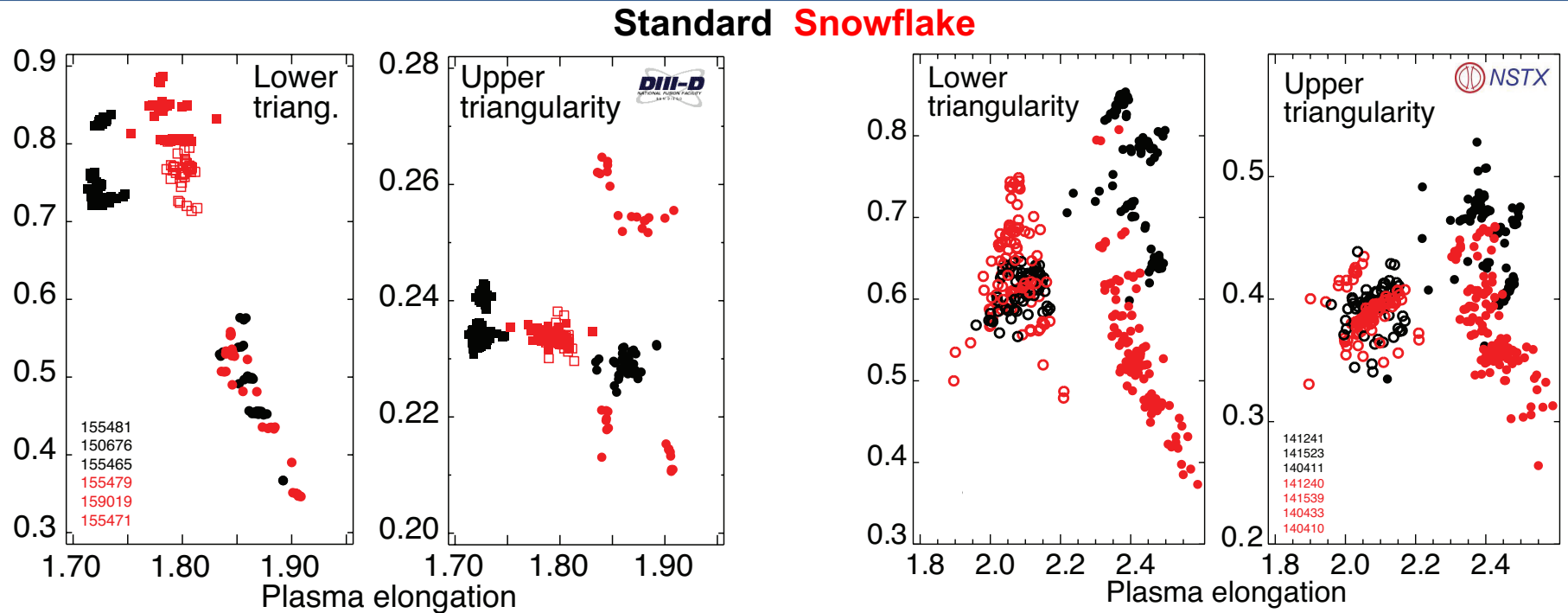
- $H98(y,2) \sim 1.0-1.2$, $\beta_N \sim 2$
 - Pedestal weakly affected
 - Partial outer strike point detachment
 - Destabilization of large Type I ELMs
- ELM stability can be affected by snowflake divertor configuration
 - Peeling (kink) modes driven by edge (bootstrap) current
 - Ballooning modes driven by edge pressure gradient
 - Edge E_r in SF can be affected by enhanced X-transport (ion loss in divertor region)
 - Collisionality and shaping are affected by snowflake configuration

Edge radial electric field weakly affected by snowflake divertor in NSTX and DIII-D

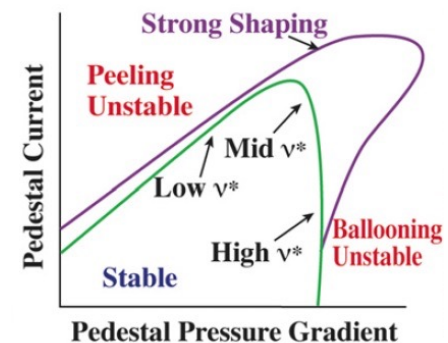


- E_r well depth and location may affect shear flow \rightarrow L-H transition
- In DIII-D, E_r well $\sim 10\%$ deeper (from profile analysis and NEO)
- In NSTX, edge E_r (as function of d_{xx}) also greater by 10-20 %
 - From edge force balance $E_r = -(v \times B)_r + \text{grad } p / Z_{\text{eff}}$ and v , p measurements

Plasma shaping enhanced as a result of transition from standard to snowflake divertor



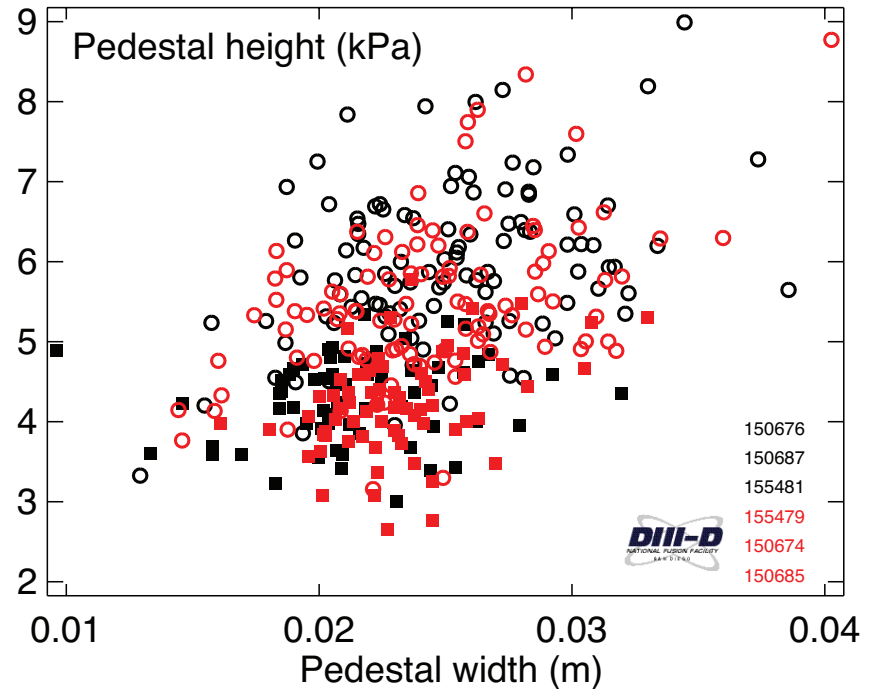
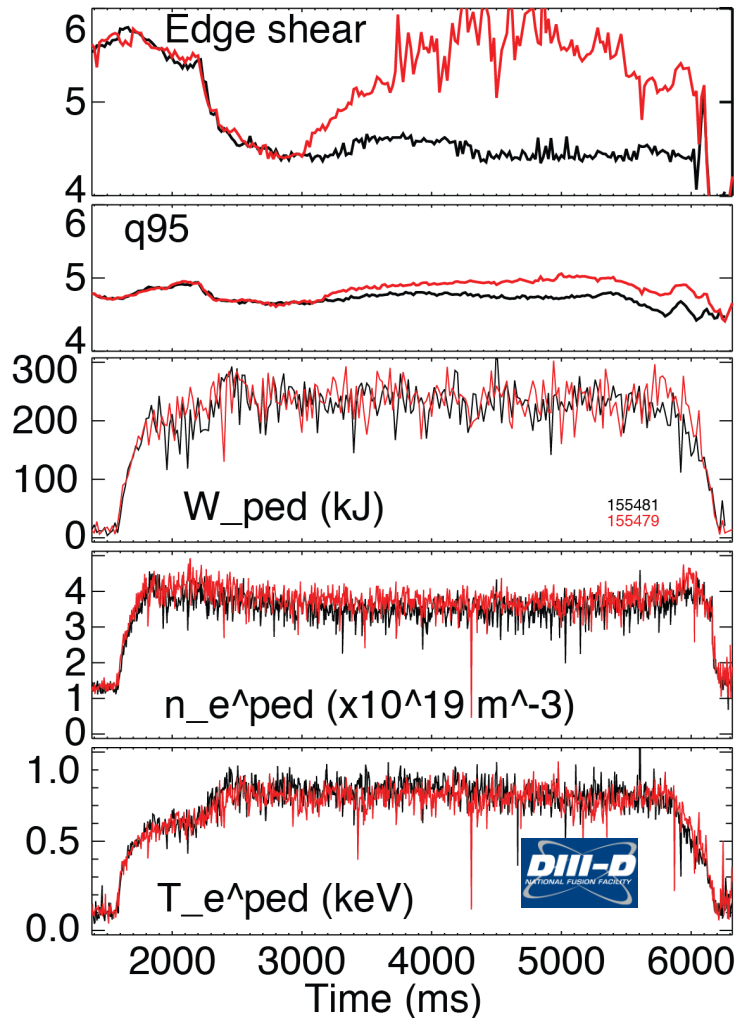
- DIII-D and NSTX: stronger shaping with SF (higher κ , δ)
- Stronger shaping could contribute to stabilizing certain modes
 - E.g., higher pedestal pressure – stabilizing effect on ideal ballooning modes



P. Snyder NF 2009

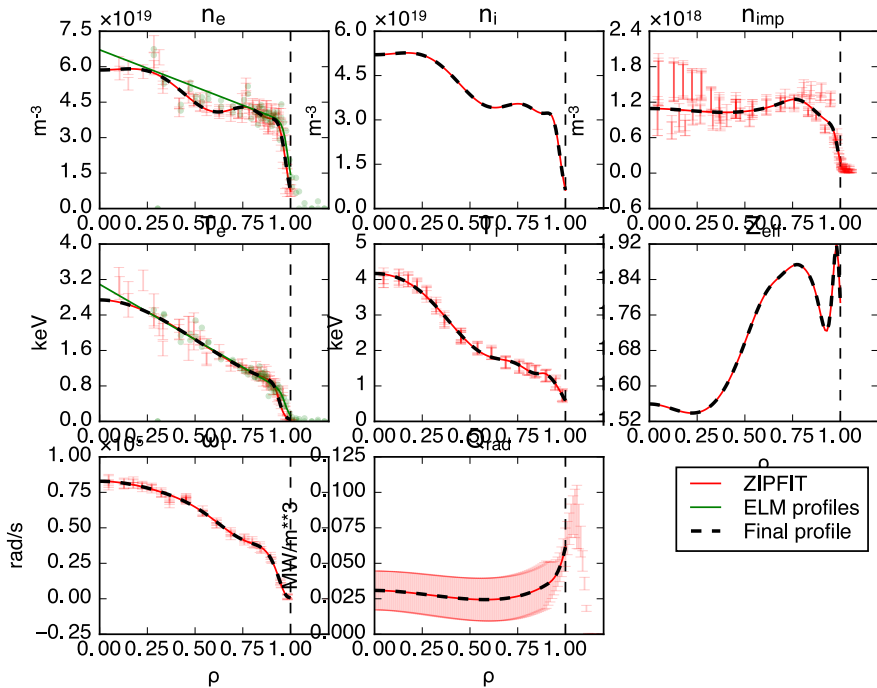
Pedestal kinetic profiles and structure are practically unaffected in DIII-D with snowflake divertor

Standard **Snowflake**

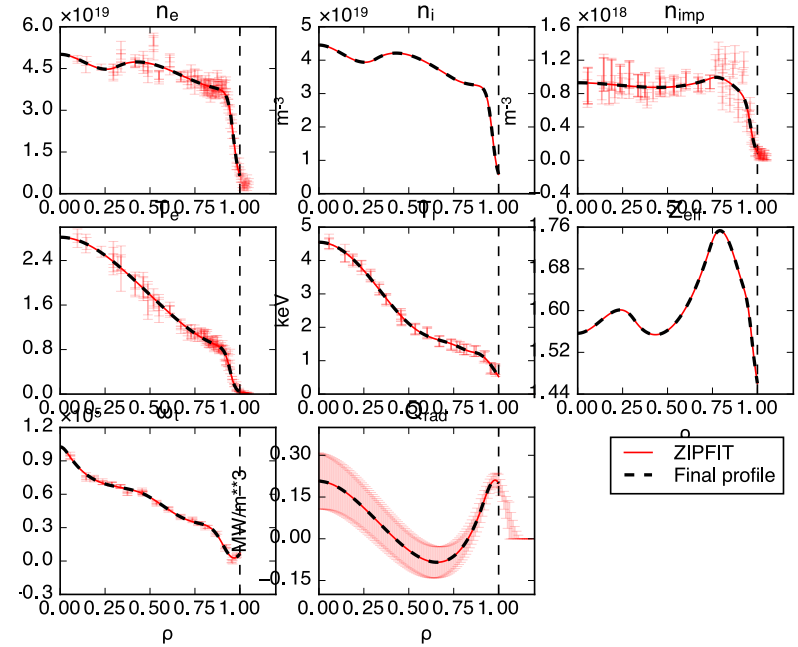


- Shear95, q95 increased by up to 30%
- Medium-size type I ELMs
- Pedestal height $\sim W_{ped}, W_{MHD}$
- Pedestal width $\sim \beta_p^{ped}$

DIII-D profiles



Standard

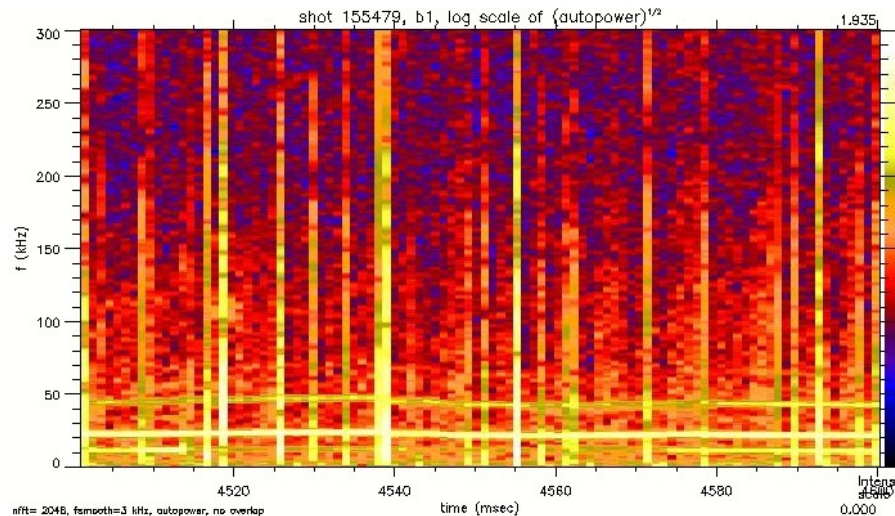
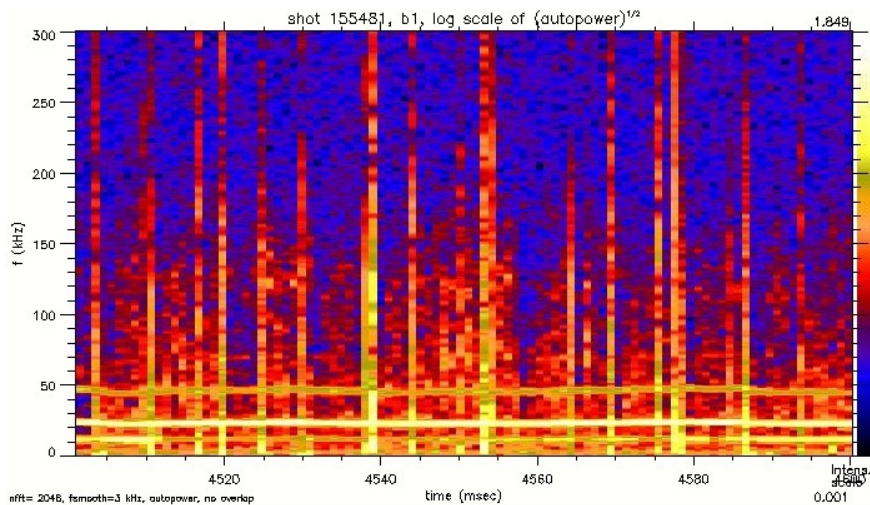
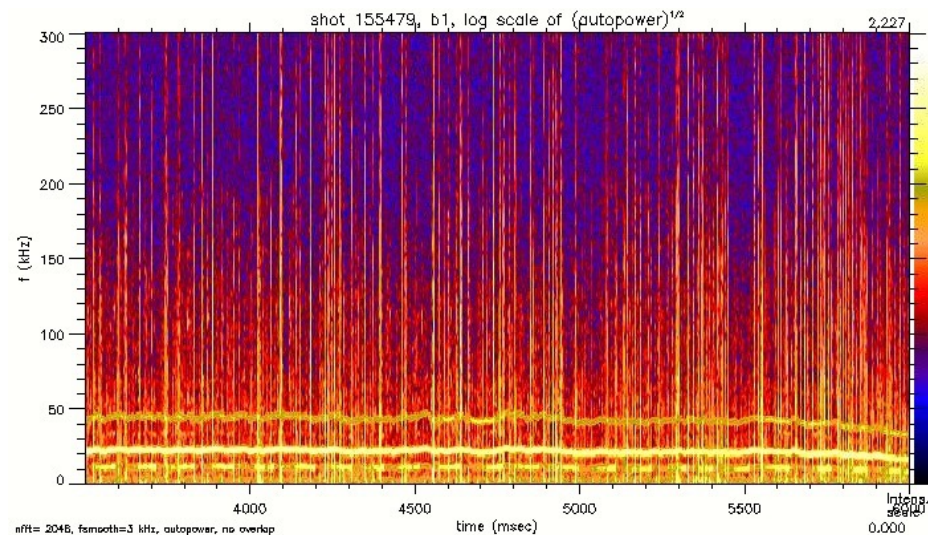


Snowflake

No significant difference in midplane between-ELM magnetic fluctuations between standard and snowflake configuration H-modes

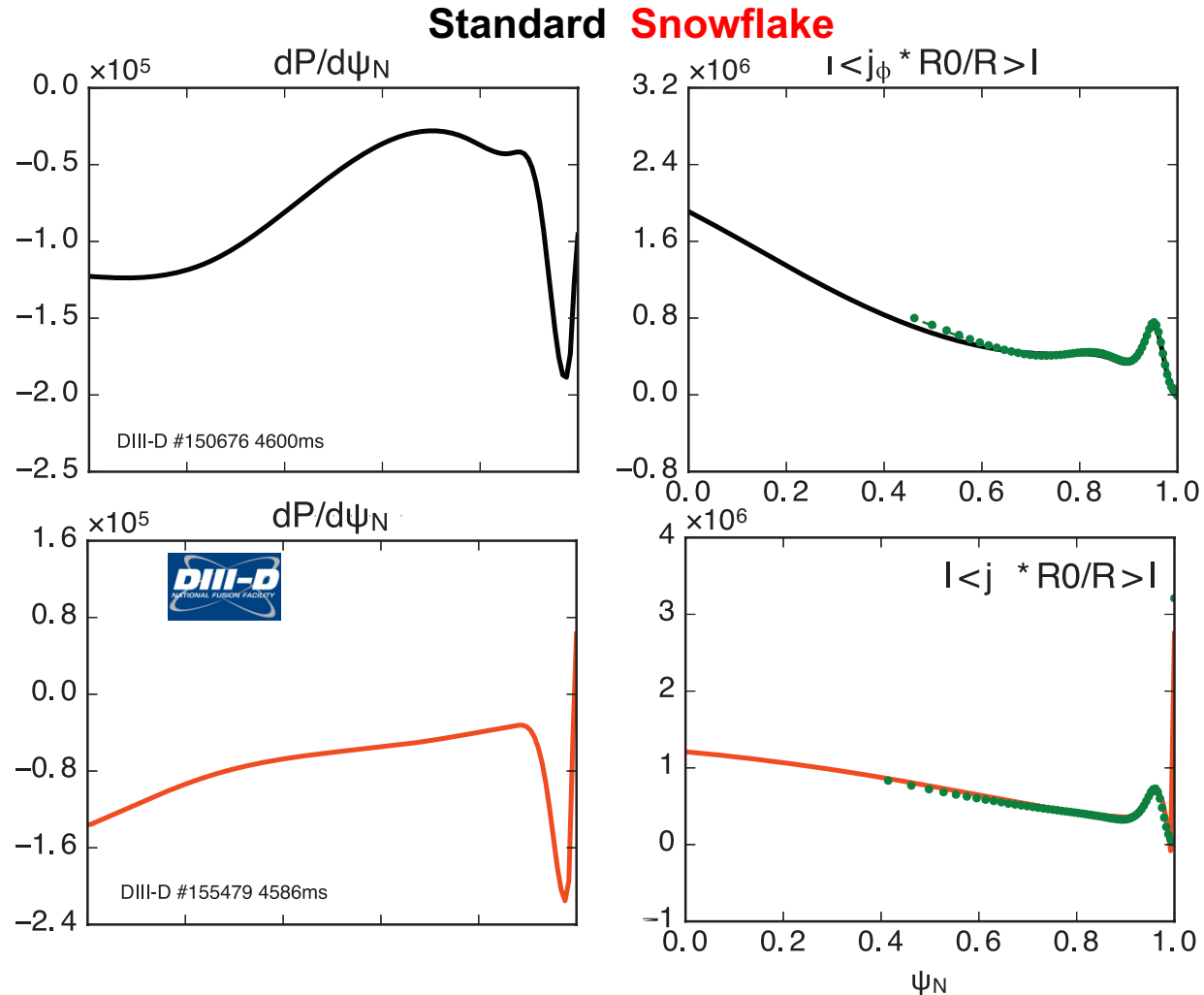


- Mirnov probe at R=167 cm, z=0 cm
- FFT autopower spectrograms
- Slightly higher level of broadband magnetic fluctuations with snowflake



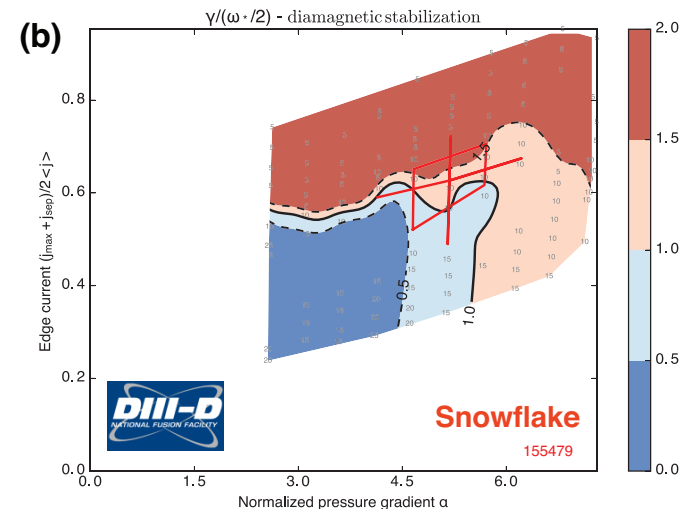
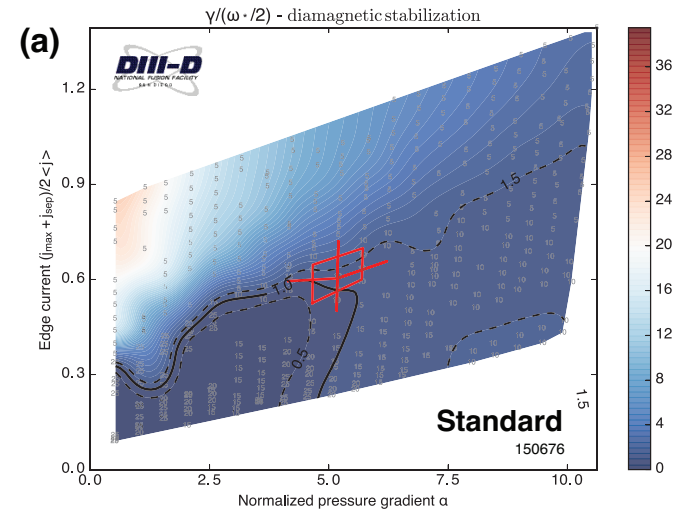
Snowflake divertor weakly affects edge pressure gradient and edge current in DIII-D

- Profiles analyzed with OMFIT
- Kinetic EFITs obtained
 - E_r self-consistently calculated by NEO
 - Fast ion pressure included from ONETWO
 - Edge current density also includes bootstrap current from NEO

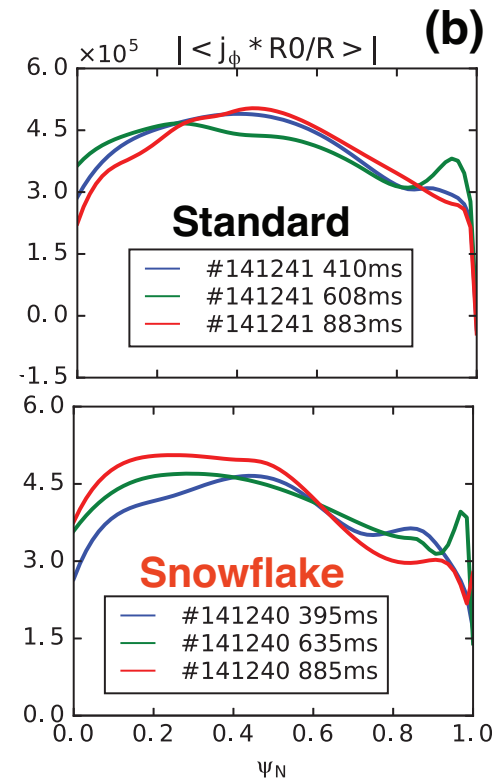
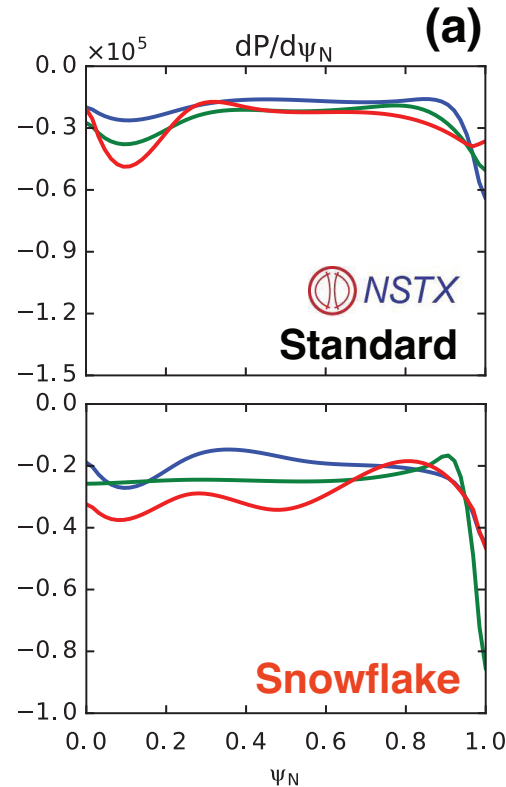
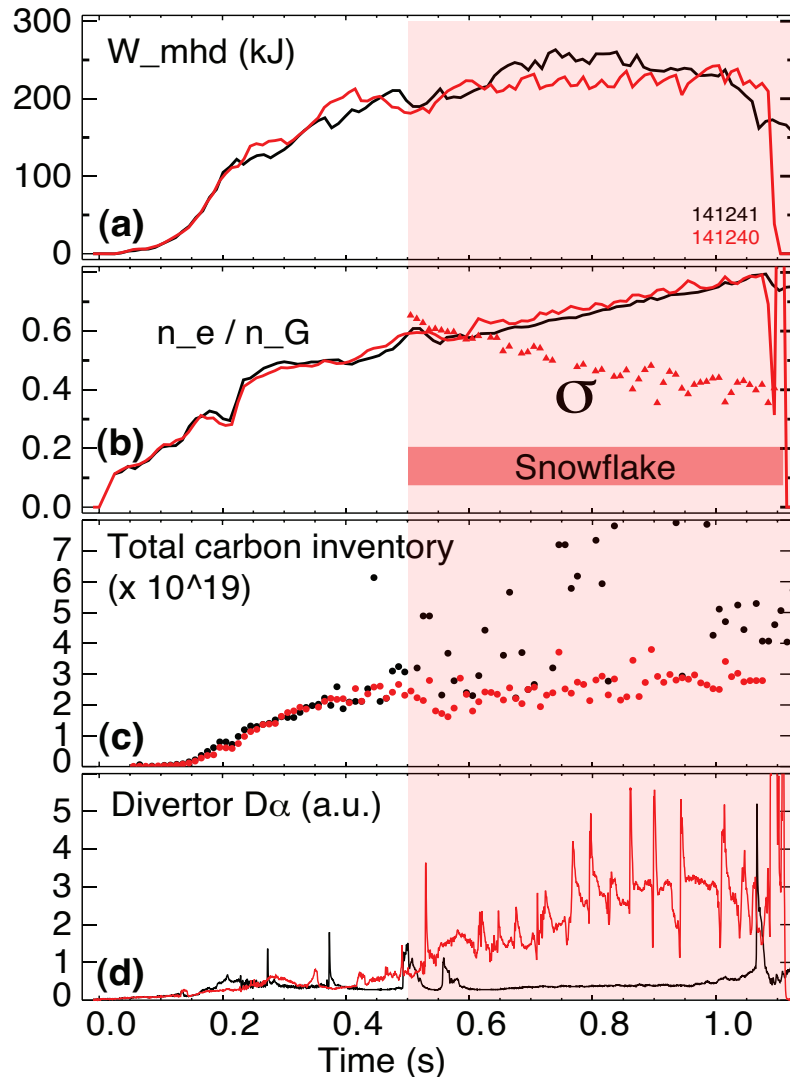


Weak changes in ELM regime with SF are consistent with ELITE calculations in DIII-D

- With both Standard and SF divertors, pedestal at the current-limiting side of stability boundary
 - Most unstable modes $n=10, 15$
- Stability calculated by ELITE
 - SNYDER, P. B. et al., Phys. Plasmas 9 (2002) 2037.
 - WILSON, H. R. et al., Phys. Plasmas 9 (2002) 1277.
- Pedestal current and pressure gradient operating space by VARYPED



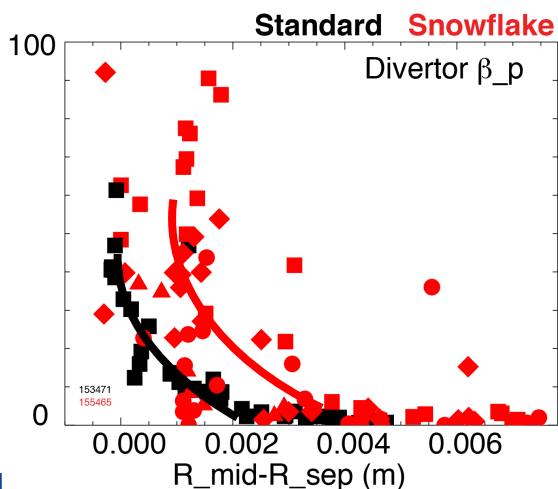
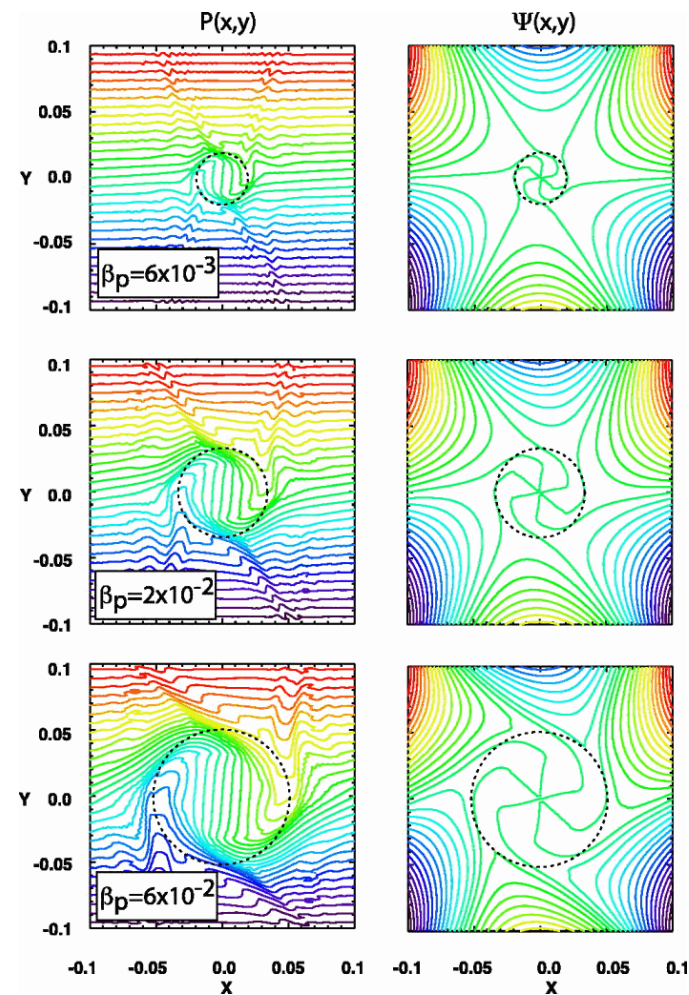
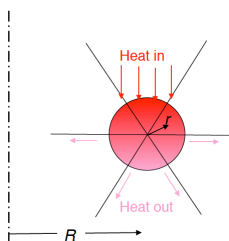
In NSTX, large ELMs destabilized with snowflake formation



- With SF formation both $dP/d\psi$ and $J(\psi)$ first increase, then relax in radiative SF phase

Convective plasma mixing driven by null-region instabilities may modify particle and heat transport in snowflake especially during ELMs

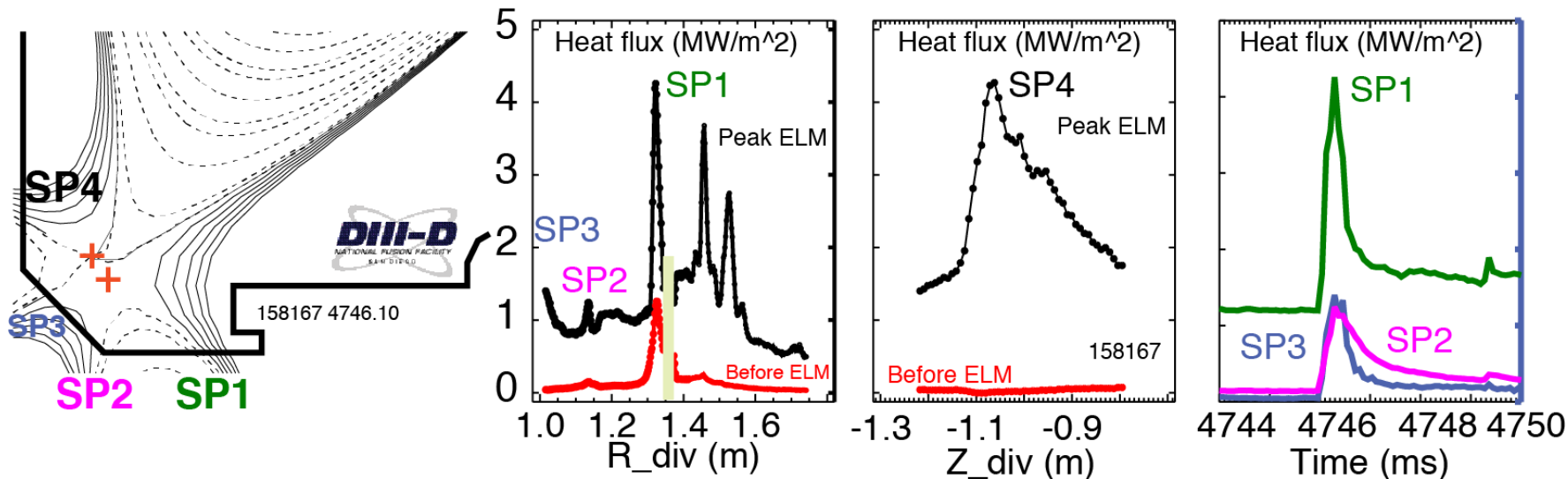
- Flute-like, ballooning and electrostatic modes are predicted in the low β_p region
 - $\beta_p = P_k/P_m = 8\pi P_k/B_p^2 \gg 1$
 - Loss of poloidal equilibrium
 - Fast convective plasma redistribution
 - Especially efficient during ELMs when P_k is large



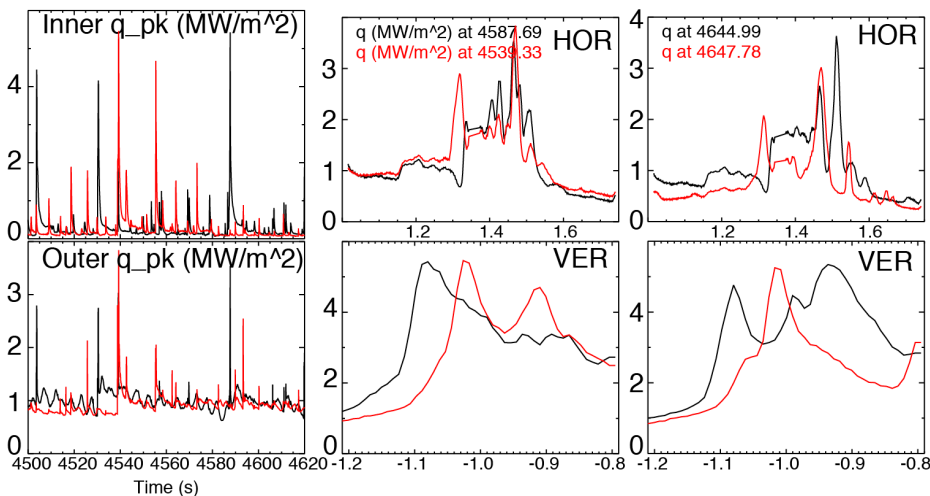
- Divertor null-region β_p measured in DIII-D divertor
 - In snowflake, broader region of higher $\beta_p \gg 1$
 - Cf. SOL $\beta_p \sim 0.01$
 - Higher X10 during ELMs

D. D. Ryutov et. al, IAEA 2012; Phys. Scripta 89 (2014) 088002
 M. V. Umansky and D. D. Ryutov, Phys. Plasmas 23, 030701 (2016)

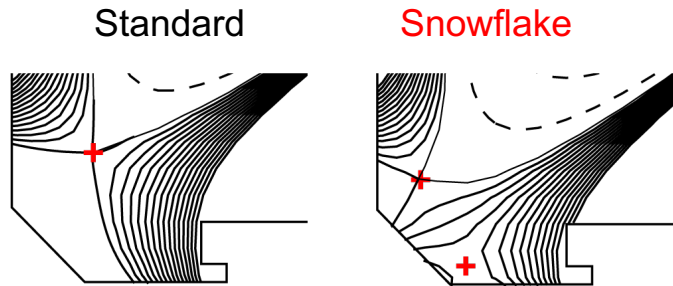
In DIII-D snowflake divertor, ELM heat is shared over additional strike points, peaks less (cf. st.div.)



- In standard divertor, inner divertor receives less or equal heat than the outer divertor (cf. JET, ASDEX)
- In both standard and SF divertors, a large fraction of ELM heat is deposited outside of divertor SOL and not affected by divertor magnetic configuration



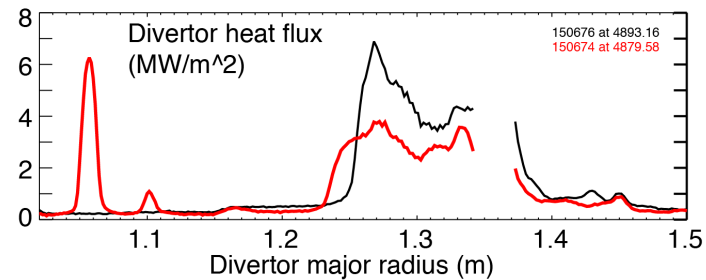
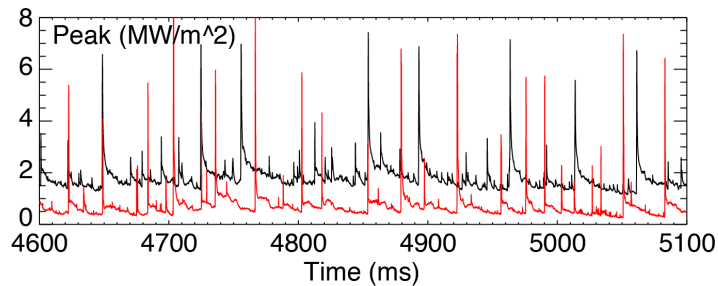
In DIII-D, Type-I ELM heat loads reduced in D_2 -seeded (partially detached) snowflake divertor



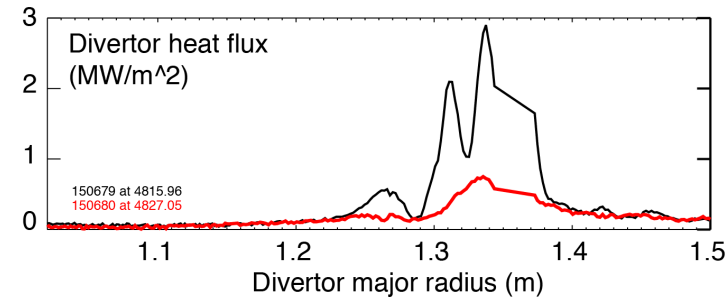
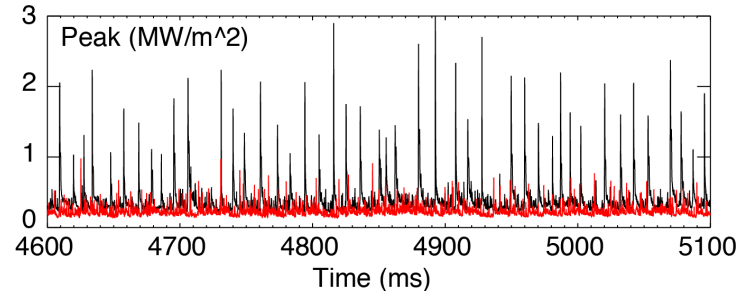
- At lower density, heat flux channels close to primary and second separatrices during ELMs
 - Additional strike points
- At high density (partial detachment), ELM heat flux significantly reduced
 - 50-75 % lower than in standard partially detached

$n_e/n_G = 0.45$

Standard Snowflake

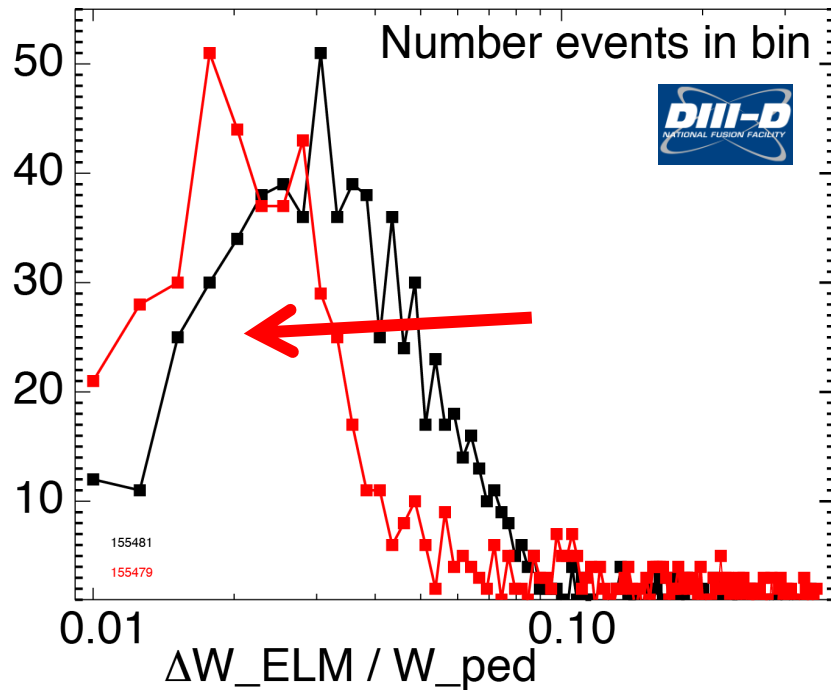


$n_e/n_G = 0.60$

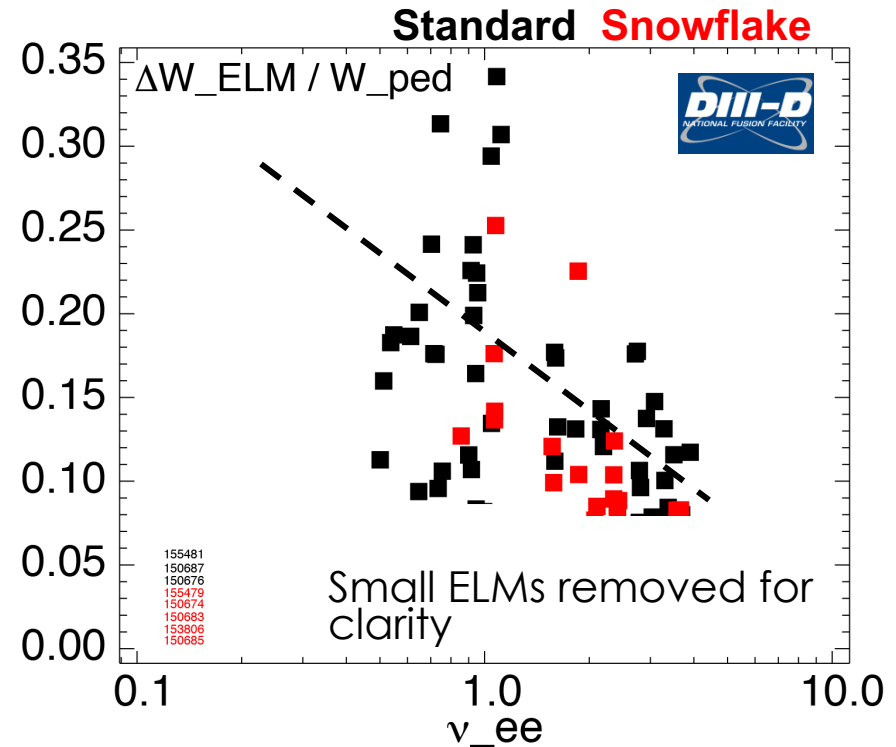


Snowflake divertor reduces ELM energy, ELM power loss scales with collisionality (also reduced)

Standard Snowflake



- Both ΔW_{ELM} and $\Delta W_{ELM}/W_{ped}$ weakly reduced
- Mostly for $\Delta W_{ELM}/W_{ped} < 0.10$



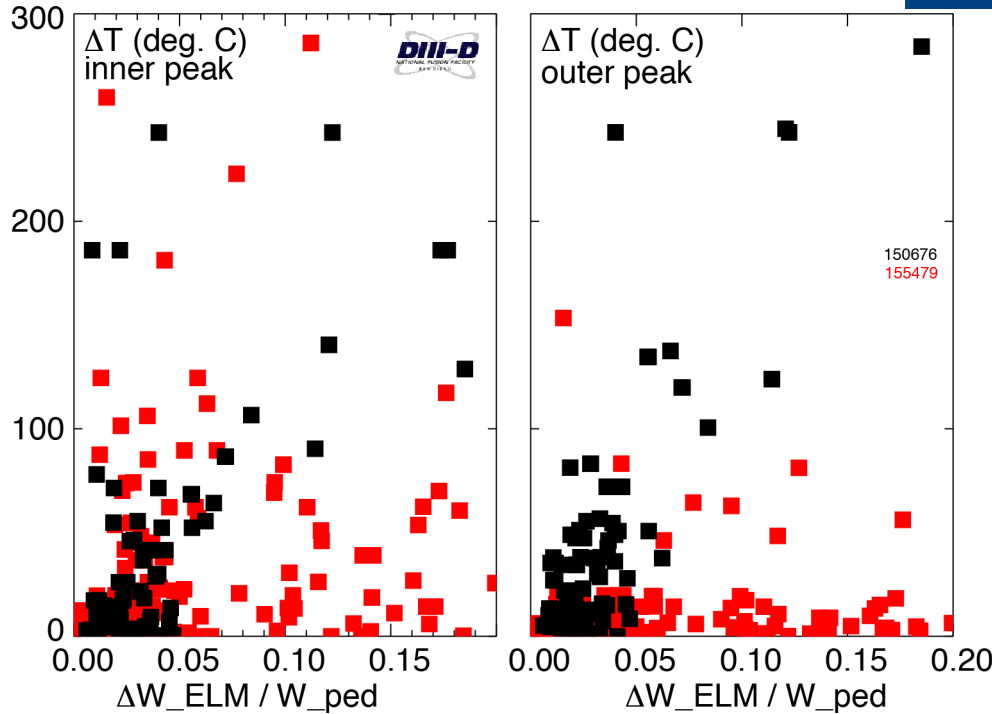
- Increased collisionality with snowflake $\nu_{ped}^* = \pi R q_{95} / \lambda_{ee}$

Snowflake divertor reduces ELM divertor surface heating (peak heat flux), increases ELM wetted area

Standard **Snowflake**

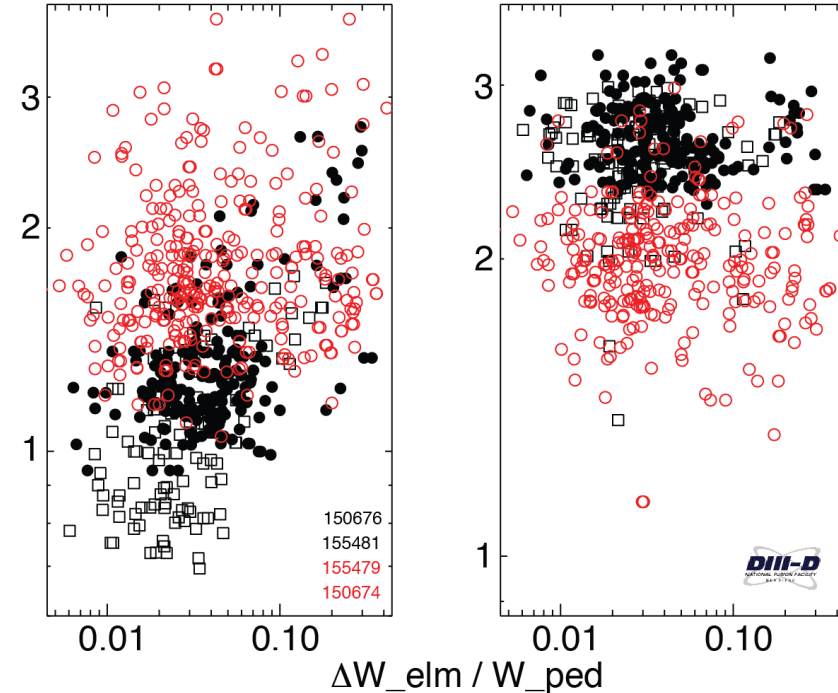


Standard **Snowflake**



A_{wet} (m²) - Outer

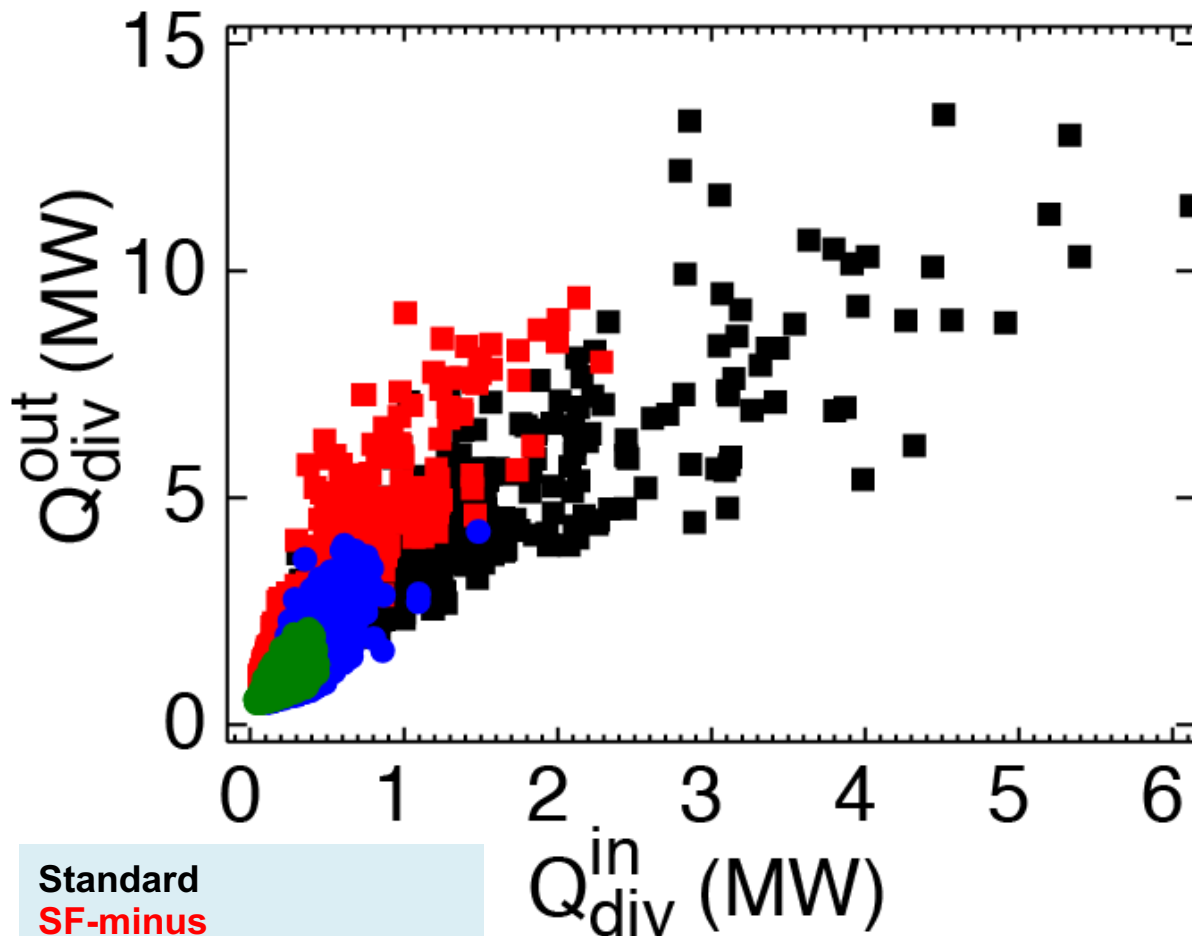
A_{wet} (m²) - Inner



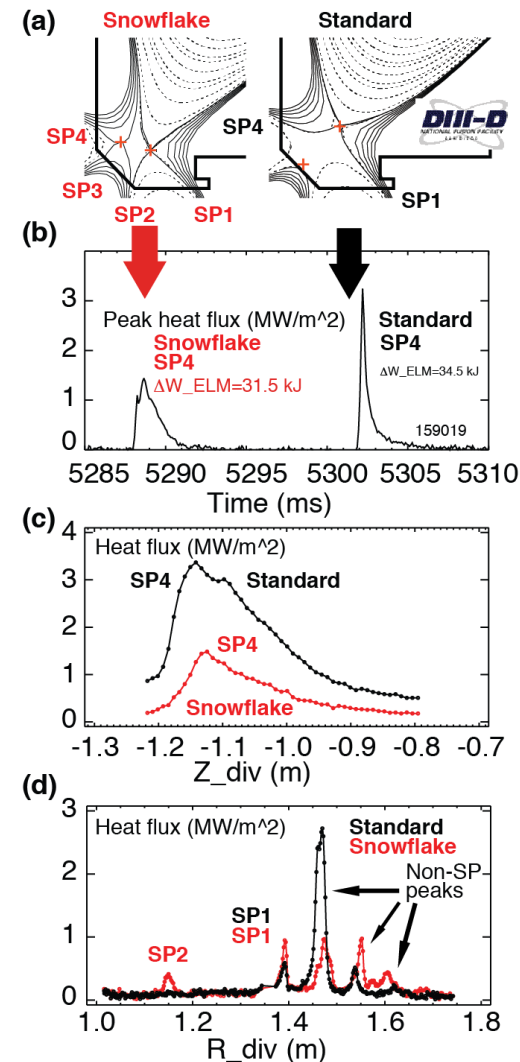
- $\Delta t_{surf} \sim E_{ELM} / (A_{wet} \tau_{heat})^{1/2}$
- Increased $\tau_{ELM} = L_{II} / c_{s,ped}$, τ_{heat}
- Reduction of ΔT and q_{peak} from larger ΔW_{ELM} ELMs (higher ion dynamic pressure) may suggest SF null-region convection

- $A_{wet} = P_{div} / q_{peak}$
- Outer divertor A_{wet} increased (due to spreading over add'l strike points)
- Inner divertor A_{wet} decreased

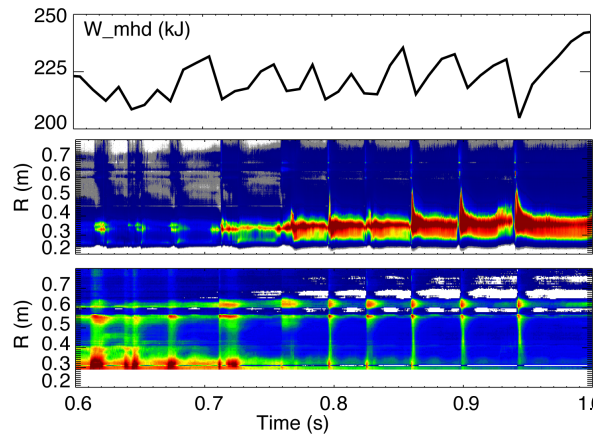
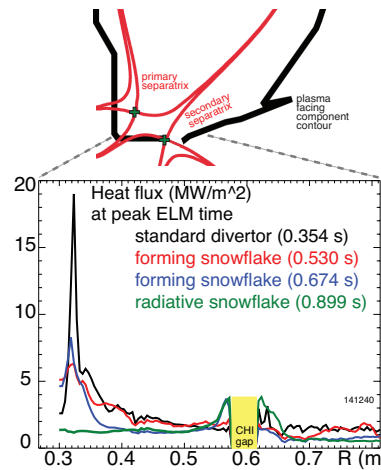
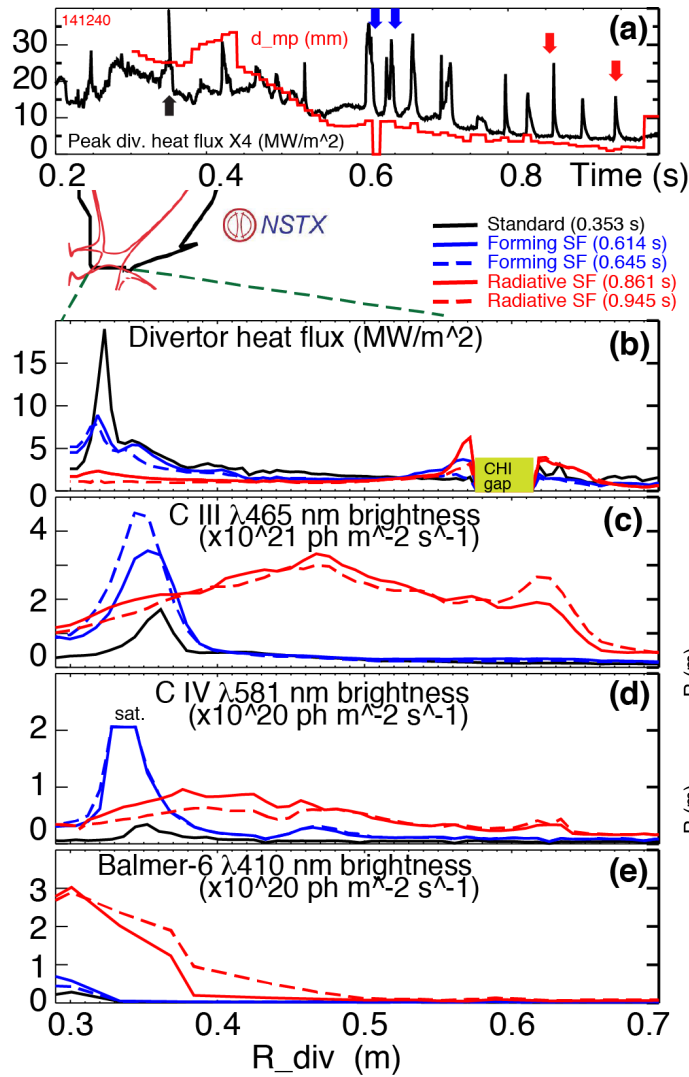
High-field-side snowflake-minus can be effectively used to mitigate inner divertor heat



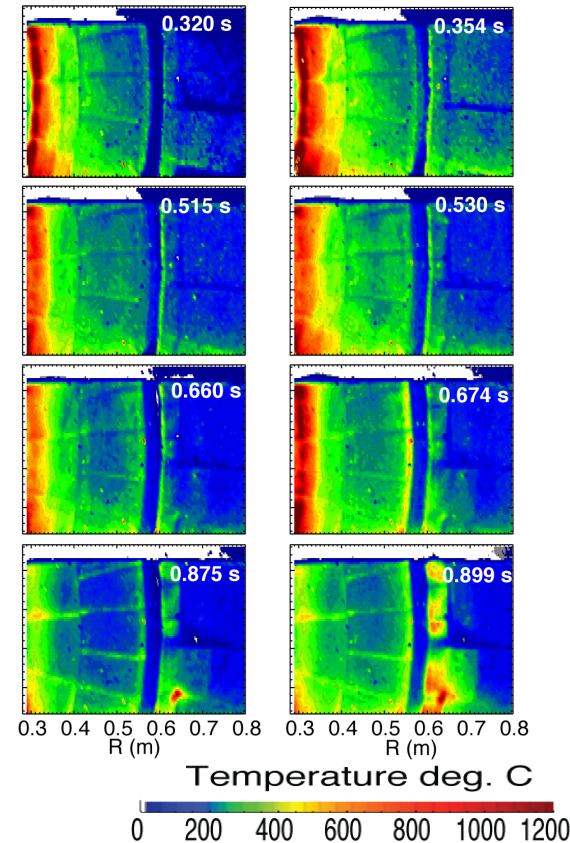
Standard
 SF-minus
 Rad. Standard
 Rad. SF-minus



Radiative snowflake divertor effectively buffers ELMs in NSTX, no excessive tile leading edge heating due to shallow angles (q_{\parallel})



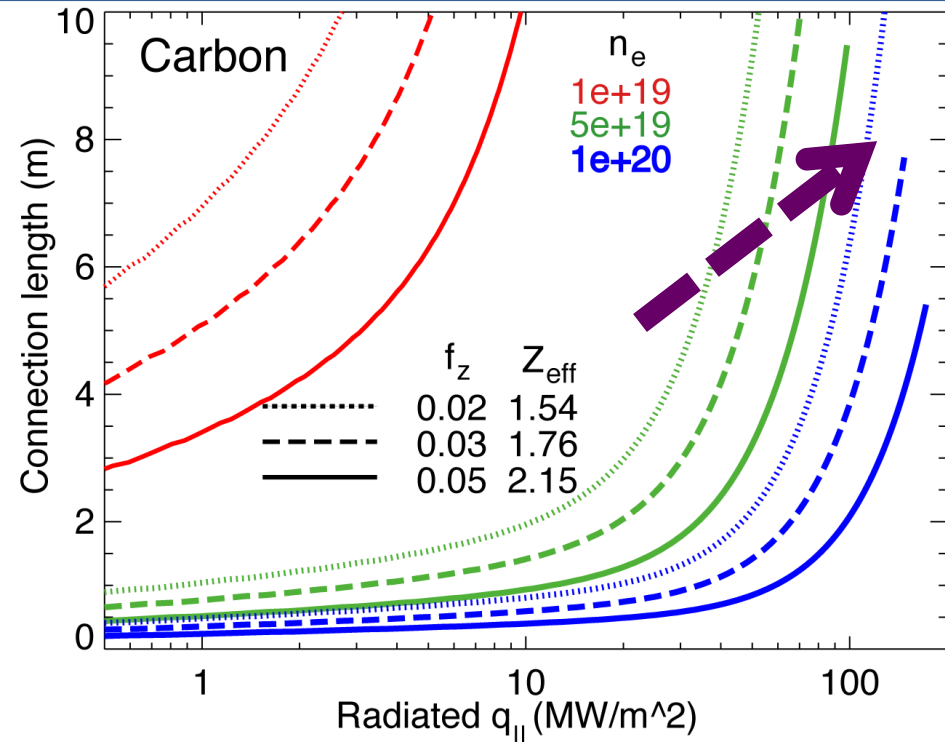
Steady-state At ELM peak



- Three phases: standard divertor, forming SF (q reduction), Radiative SF (q buffering)

1D modeling indicates power and momentum losses are increased in snowflake divertor

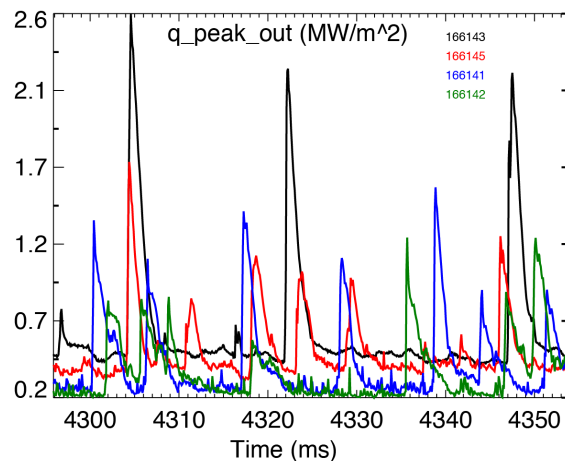
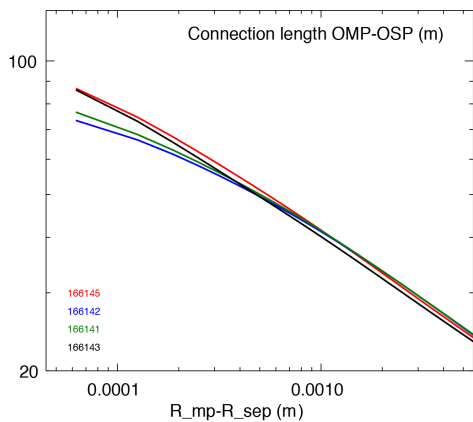
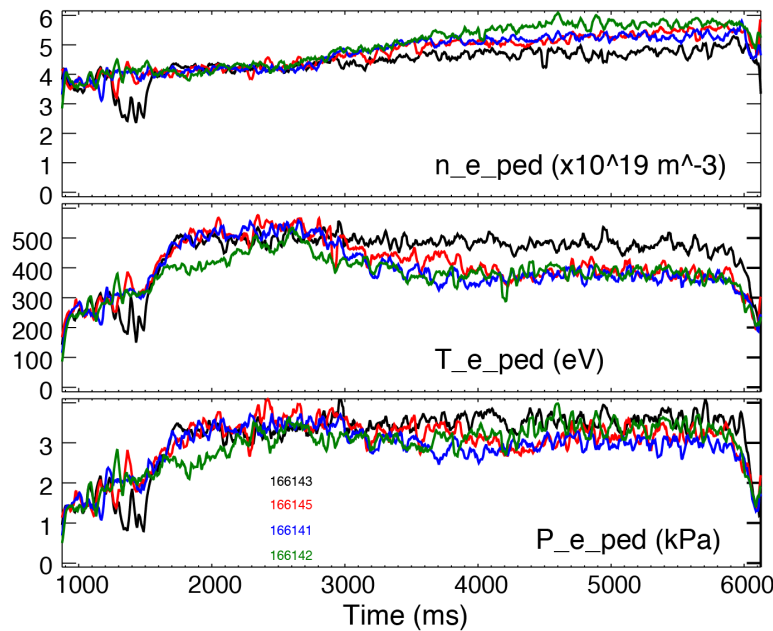
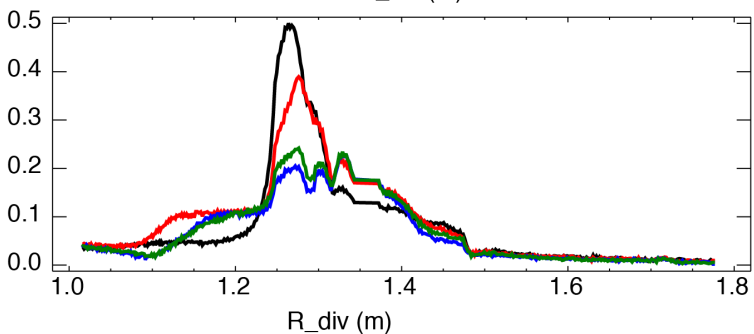
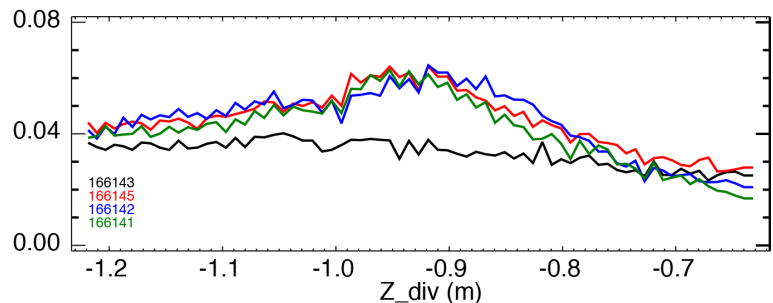
- 1D divertor detachment model by Post
 - Electron conduction with non-coronal carbon radiation
 - Max $q_{||}$ that can be radiated as function of connection length for range of f_z and n_e
- Three-body electron-ion recombination rate depends on divertor ion residence time
 - Ion recombination time: $\tau_{ion} \sim 1-10$ ms at $T_e = 1.3$ eV
 - Ion residence time: $\tau_{ion} \leq 3-6$ ms in standard divertor, x 2 in snowflake



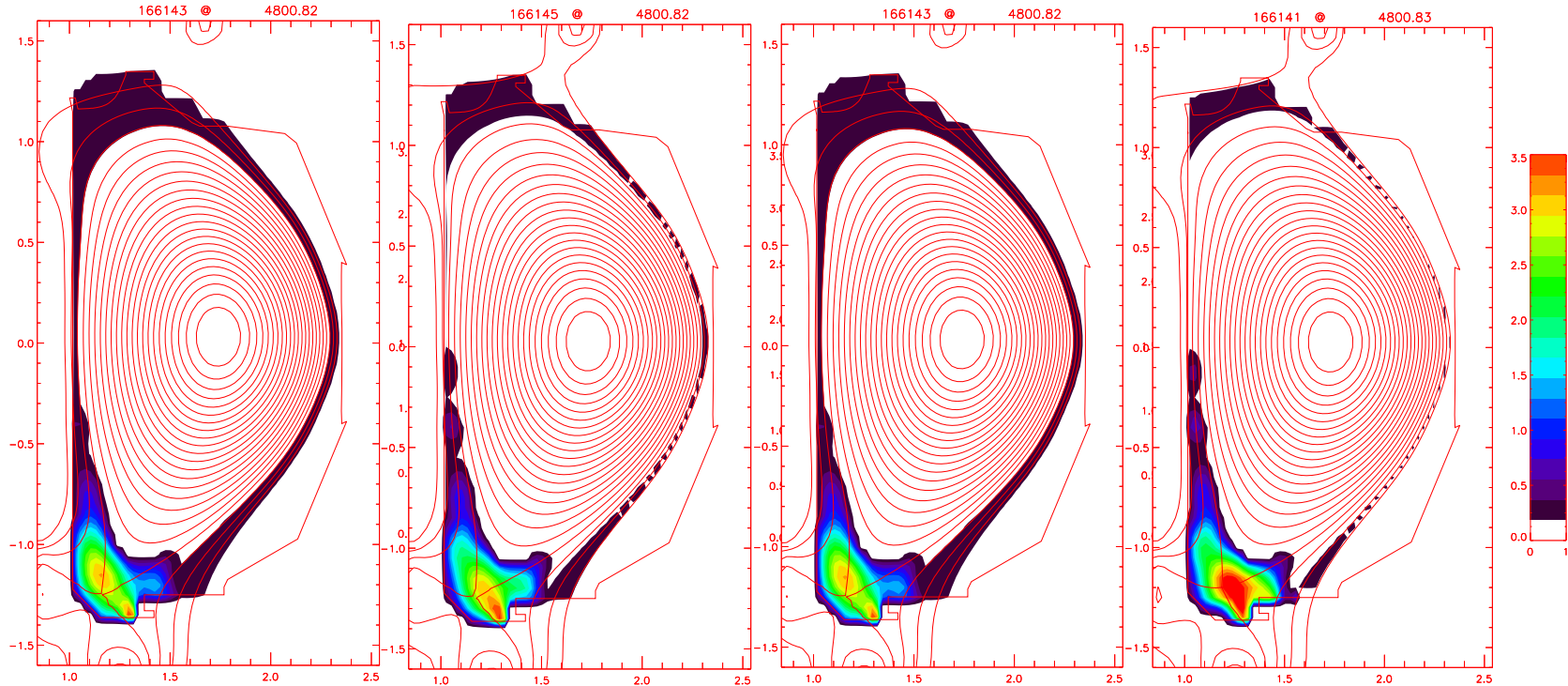
$$q_{||} = -\kappa_0 T_e^{5/2} \frac{\partial T_e}{\partial x}$$

$$\frac{\partial q_{||}}{\partial x} = -n_e n_z L_Z(T_e)$$

CD₄-seeded snowflake divertor development at DIII-D

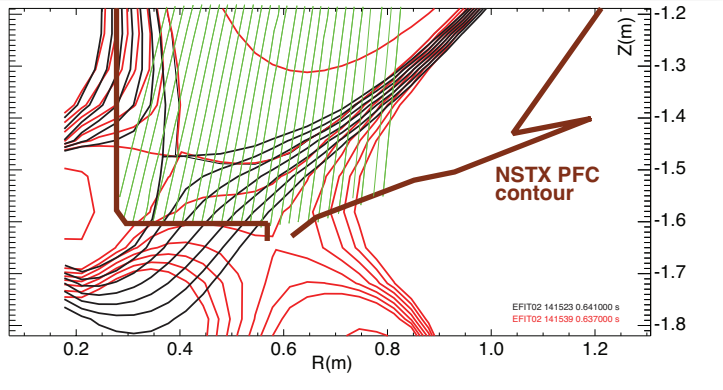


CD₄-seeded snowflake divertor development at DIII-D



- 1.2 MA, 5 MW NBI heated H-mode discharges

Different ELM and impurity regimes due to divertor geometry and CD₄



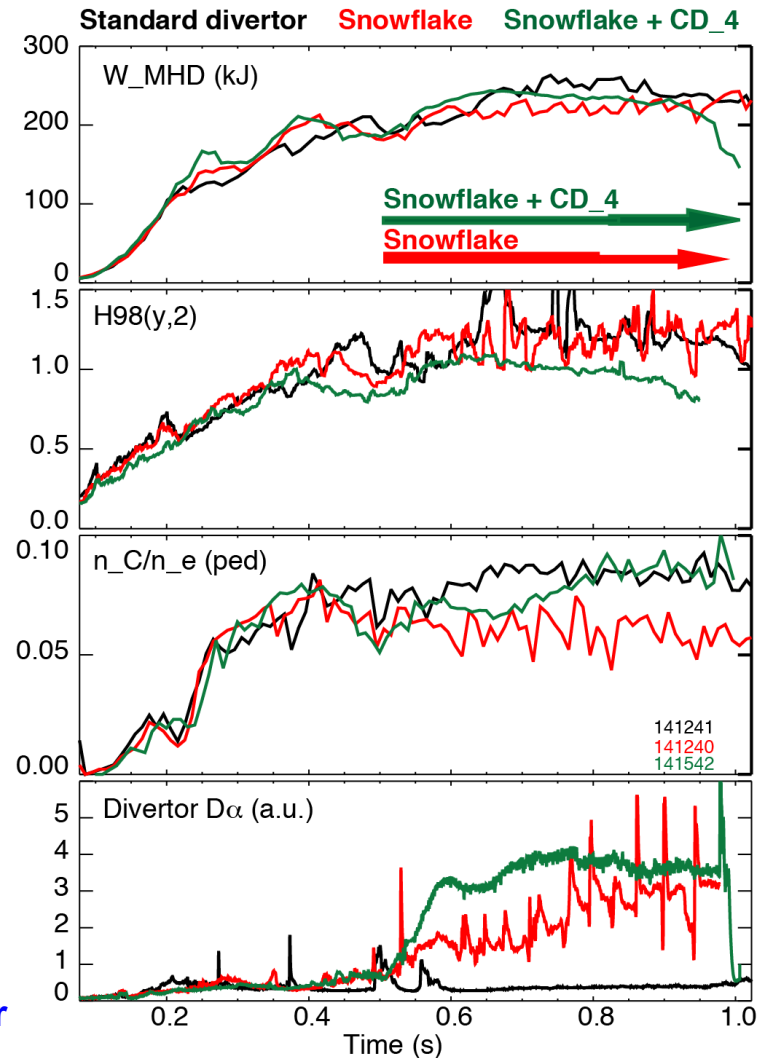
- High-performance H-mode with reduced divertor heat flux
- ELM and impurity control

	Lithium conditioning, no CD ₄ ,	Lithium conditioning, divertor CD ₄ inj.	Lithium conditioning, midplane CD ₄ inj. from SGI
Standard divertor	ELMs stabilized, Impurity accumulation 141523, 141524, 141537	Singular ELMs, Impurity accumulation 141532	ELMs stabilized 141534, 141535
Snowflake-minus divertor	Type I ELMs, $f_{ELM}=12-35$ Hz, $\Delta W_{MHD}/W_{MHD}\sim 0.05-0.1$ 141240, 141539	Singular ELMs, then ELMs stabilized 141542	

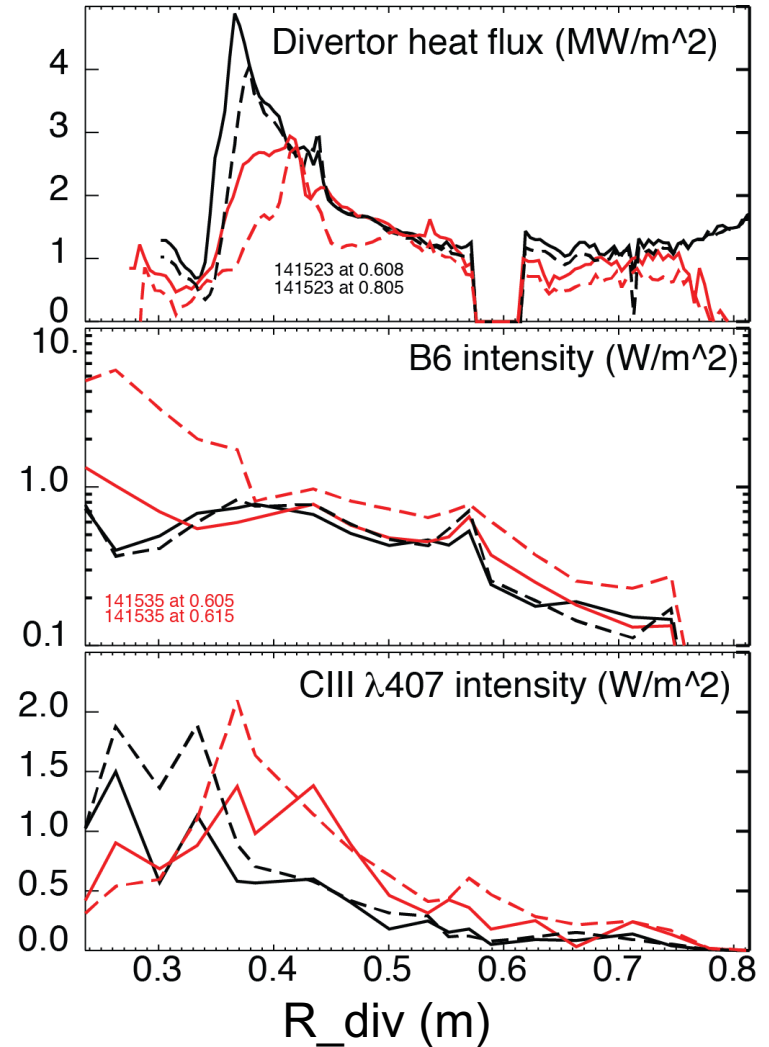
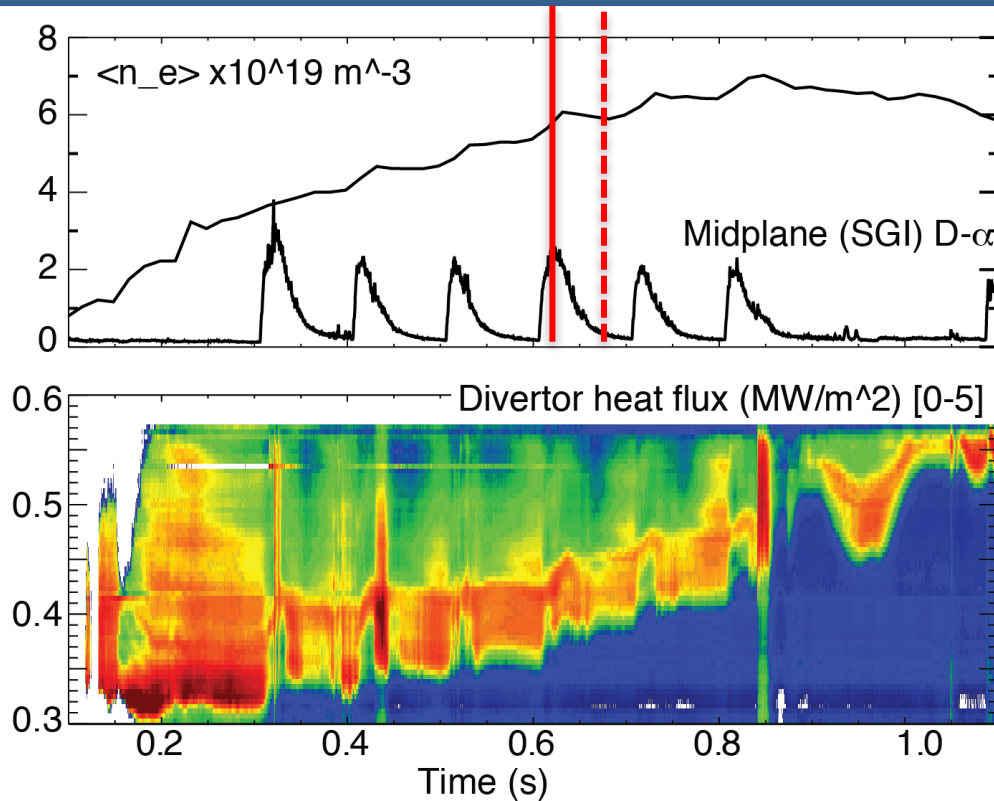
10-20% reduction in confinement (H_{98} and W_{MHD}) in H-mode with CD_4 -seeded snowflake divertor

- 0.45 T, 0.9 MA, 4 MW H-mode
- Shaping: $\kappa=2.1$, $\delta=0.8$
- Core temperature:
 - $T_e \sim 0.8-1$ keV
 - $T_i \sim 1$ keV
- $\beta_N \sim 4-5$
- $H_{98}(y,2) \sim 1$ (from TRANSP)
- $P_{SOL}=3$ MW
- Magn. Balance: $drsep=6-7$ mm (cf. $\lambda_{SOL} \sim 6$ mm)
- B x grad B toward lower divertor

Reference
Snowflake
 Radiative divertor
Snowflake+CD₄

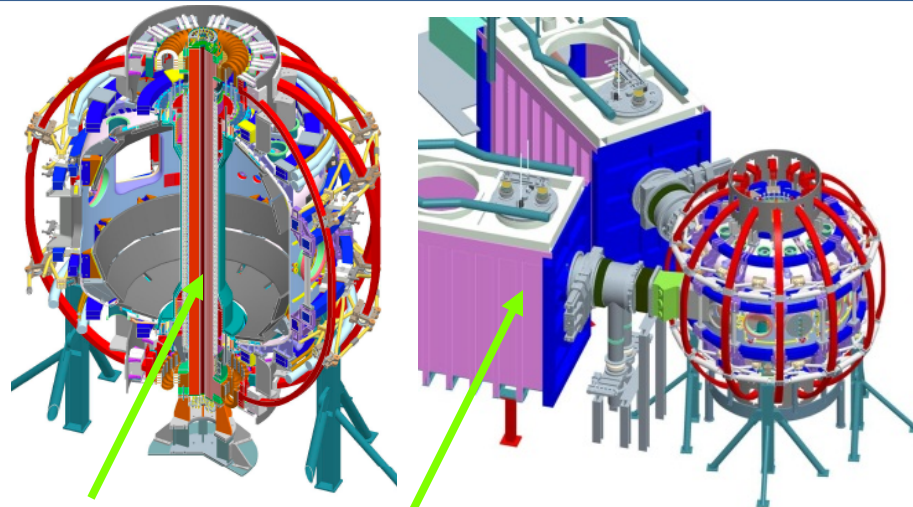


CD₄ puffing from midplane SGI produces dynamic partial detachment only during SGI pulses



- SGI produced intense CD₄ pulses resulting in pulsed upstream density

Snowflake divertor is a leading heat flux mitigation candidate for NSTX Upgrade

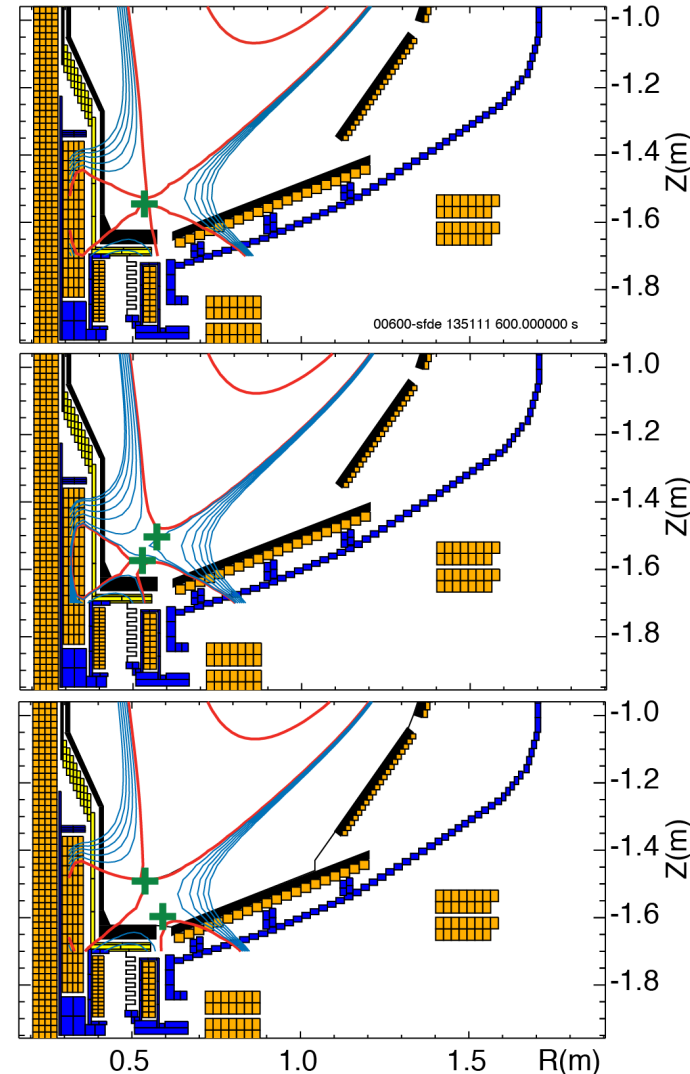


New center-stack 2nd neutral beam

B_T	→ 1 T	P_{NBI}	→ 12 MW
I_p	→ 2 MA	pulse	→ 5 s

J. E. Menard et. al, Nucl. Fusion 52 (2012) 083015

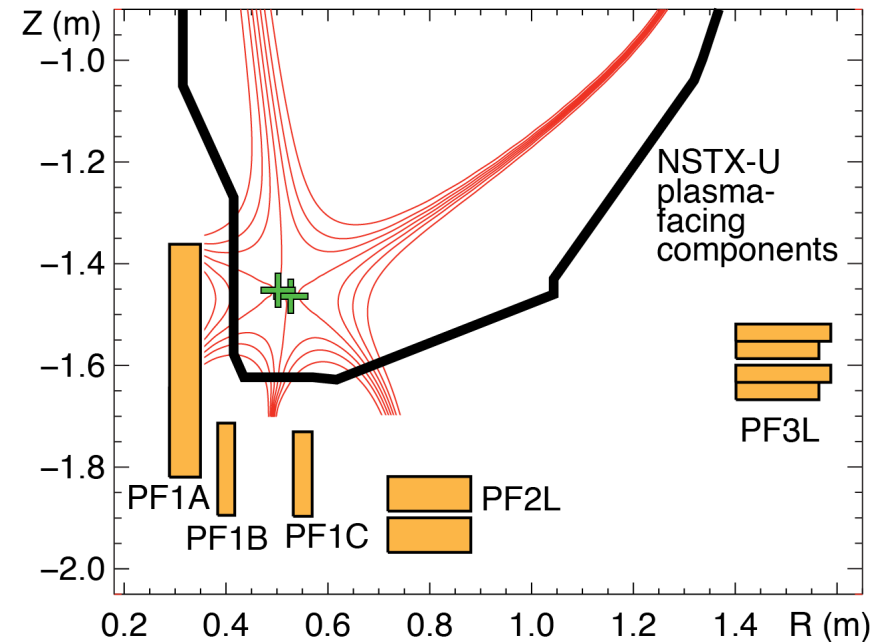
- NSTX-U Mission elements:
 - Advance ST as candidate for Fusion Nuclear Science Facility
 - **Develop solutions for the plasma-material interface challenge**
 - Explore unique ST parameter regimes to advance predictive capability for ITER
 - Develop ST as fusion energy system



Snowflake divertor equilibria obtained with ISOLVER and realistic divertor coil currents



- Four divertor coils in NSTX-U
 - Only three coils in initial years
- ISOLVER used for equilibria
 - Predictive free-boundary axisymmetric Grad-Shafranov equilibrium solver
 - Input: normalized profiles (P , I_p), boundary shape
 - Match a specified I_p and β from an NSTX shot
 - Output: magnetic coil currents



Divertor coil	Current limits (kA)	Standard configuration currents (kA)	Near-exact SF configuration currents (kA)	SF-plus configuration currents (kA)	SF-minus configuration currents (kA)
PF1A	19	2.3	3.1	2.8	3.2
PF1B	13	0	0	0	0
PF1C	-8 / + 16	0.4	-1.4	-0.97	-1.3
PF2L	15	1.0	6.6	5.4	6.2

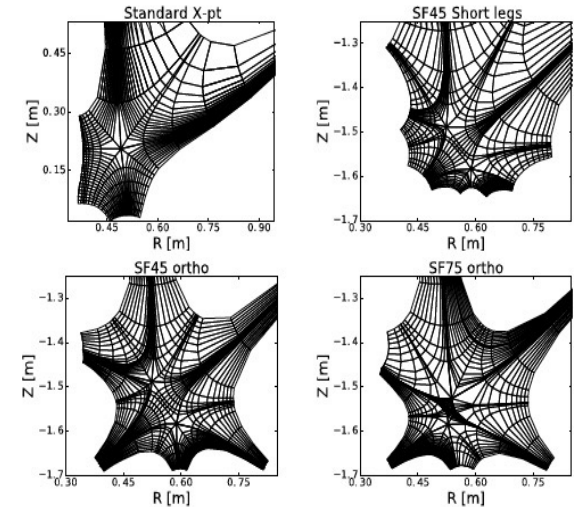


Edge modeling predicts significant heat flux reduction with radiative snowflake divertor

- New UEDGE grid generator for nearly-arbitrary divertor configuration
- Multi-fluid code UEDGE
 - $B_t = 1.0$ T, $I_p = 2$ MA, $P_{\text{SOL}} = 9$ MW
 - NSTX-like transport $\chi_{i,e} = 2-4$ m²/s, $D = 0.5$ m²/s

O. Izacard,
NP10.00010

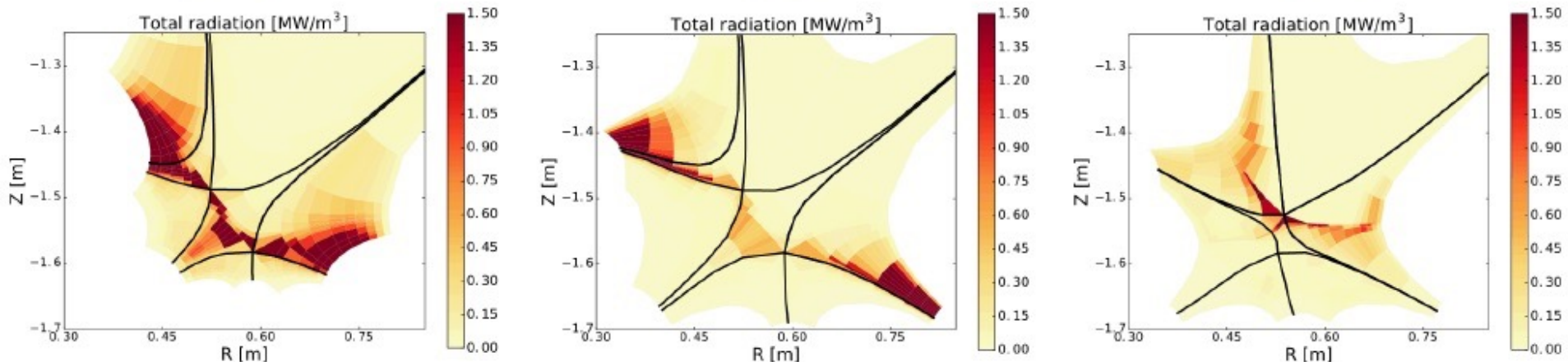
Standard **Snowflake**



SF45

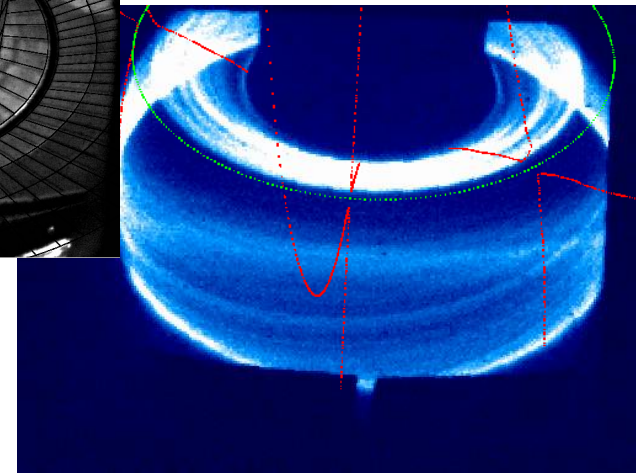
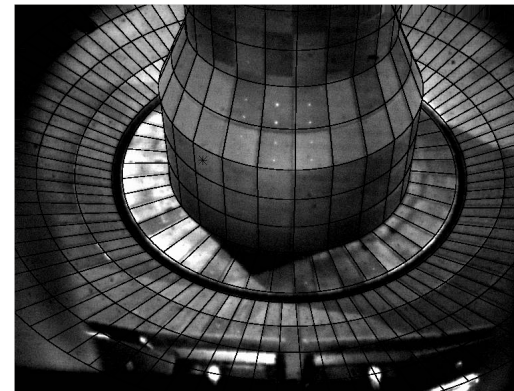
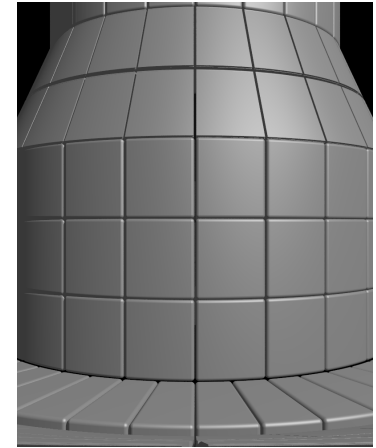
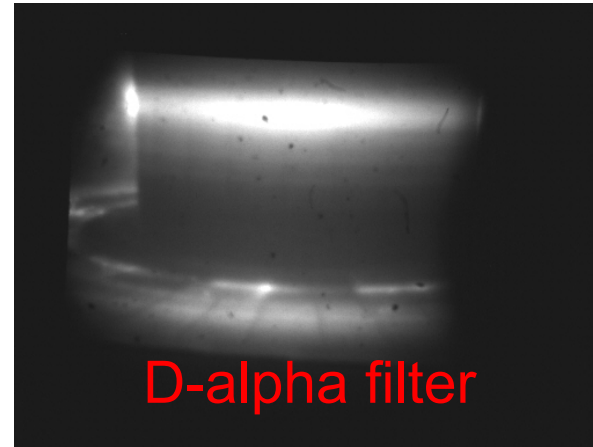
SF45

SF75



Fast filtered visible camera will enable divertor emission distribution and turbulence imaging in NSTX-U

- Vision Research Phantom camera v1211
- 1280x800 pixels
- Pixel size 28x28 micron
- Chip size 35.8 x 22.4 mm
- Planned divertor turbulence studies
 - Filament imaging
 - Turbulence metrics

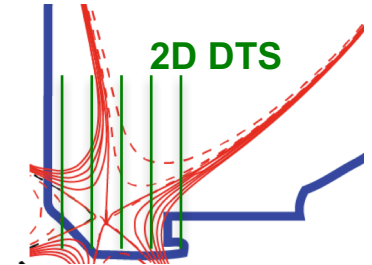


**F. Scotti,
NP10.00028**

Resolution	Max kfps	Max rec time (s)
1280x800	12.6	1.3
256x256	103.4	2.42
128x128	240.3	3.85
128x64	415.1	4.06
128x32	571.0	5.0

Outstanding questions

- Develop real-time near-exact snowflake configuration feedback control
- Identify transport mechanisms
 - For heat and particle flux sharing between multiple strike points (inter-ELM and ELM)
 - For SOL broadening
- Identify radiation limits at high density and with seeded impurities
- Confirm particle control via cryo-pumps
- Investigate pedestal MHD stability control



Proposed DIII-D experiments with new DTS